Investigation and Development of the Quality Control of Al-Wheel Rim Production Process

by

Mert ÇETİNEL

A Dissertation Submitted to the
Graduate School in Partial Fulfillment of the
Requirements for the Degree of

MASTER OF SCIENCE

Department: Mechanical Engineering
Major: Mechanical Engineering

İzmir Institute of Technology
İzmir, Turkey

October, 2001

We approve the thesis of **Mert ÇETİNEL**.

Date of Signature

_____ **19.10.2001**

Assist. Prof. Dr. Hacer AYGÜN

Supervisor

Department of Mechanical Engineering

_____ **19.10.2001**

Prof. Dr. Zafer İLKEN

Department of Mechanical Engineering

_____ **19.10.2001**

Assist. Prof. Dr. Mustafa GÜDEN

Department of Mechanical Engineering

_____ **19.10.2001**

Assist. Prof. Dr. Murat GÜNAYDIN

Department of Architecture

_____ **19.10.2001**

Assist. Prof. Dr. Figen KÖSEBALABAN

Department of Food Engineering

_____ **19.10.2001**

Prof. Dr. Zafer İLKEN

Head of Department

ACKNOWLEDGEMENTS

It is a pleasure for the author to express his sincere gratitude to his supervisor, Assist.Prof.Dr. Hacer Aygün for her invaluable guidance, continual supports and constant encouragement throughout the course of this study.

The author is grateful to Mr. Can Demir for his suggestions and comments and to the Casting Foundry for supplying data and materials.

Finally, the author wishes to express his thanks to his family for their help and support during his studies.

ABSTRACT

With the increasing use of aluminum wheels in automotive industry, the aluminum foundry industry had to focus on the quality and reliability of the products. To produce good quality aluminum cast wheels, defects must be minimized and the quality of each production step must be controlled.

The main topic of this study was to investigate the production line of a big aluminum wheel foundry and improve the quality of production using quality control tools.

The production parameter data and real-time x-ray inspection results have been collected. Parameters of the machines that are involved with the production and the results of testing equipment and thermal analyzer have been recorded.

To obtain effective feedback during process, a proposed flow chart of the wheel production line was developed. The process parameters which have influences on the quality of wheel were determined by using Fishbone diagrams. According to the results of real-time radioscopic inspection, it was concluded that the main defects that occur on Al wheel are gas holes, porosity and shrinkage. The locations of the defects were identified with results of inspection and evaluated by using the charts. To eliminate these defects, some outstanding remedies are given in the flow chart of Al wheel production.

A predicted equation between hydrogen content and density index of gas holes in molten metal was obtained by using the Least Square Method. Analysis of variance for the single factor showed that degassing time affects the hydrogen content in the molten metal. Finally, hydrogen content and the molten metal temperature relationship was investigated by a graphical method.

ÖZ

Alüminyum jantların otomotiv sektöründe kullanımının artmasıyla alüminyum döküm endüstrisi ürünlerin kalitesi ve güvenilirliği üzerine odaklanmıştır. Yüksek kalitede alüminyum döküm jantların üretilmesi için, jantta oluşabilecek hatalar en aza indirilmeli ve üretimin her aşaması kontrol altında tutulmalıdır.

Bu çalışmanın amacı, büyük bir döküm alüminyum jant fabrikasının üretim hattı incelenerek bazı kalite kontrol araçları yardımıyla üretimin kalitesini arttırmaktır.

Deneysel çalışma süresince kontrol formları kullanılarak üretimde kullanılan çeşitli cihazlardan alınan veriler ve eş zamanlı radyoskopik muayene sonuçları değerlendirilmiştir.

Üretim süresince etkin bir geri-besleme sağlamak için jant üretim hattı için bir akış diagramı geliştirilmiştir. Neden-sonuç diagramları kullanılarak jantın kalitesini etkileyen üretim parametreleri tanımlanmıştır. Eş zamanlı radyoskopik muayene sonuçlarına göre, Al jant üzerinde genelde oluşan hatalar gaz boşlukları, porozite ve çekintidir. Bu hataların jant üzerinde oluştukları bölgelerin dağılımı grafiksel olarak gösterilmiştir. Bununla birlikte, jant üretimi için oluşturulan akış diagramında bu hataların oluşumunu önlemek için alınabilecek tedbirler üzerinde durulmuştur.

En Küçük Kareler Yöntemi kullanılarak sıvı metaldeki hidrojen miktarı ve gaz boşluklarının yoğunluk indeksi arasındaki ilişki tahminlenen ve doğruluğu ispat edilen bir denklemle gösterilmiştir. Gaz alma süresinin sıvı metaldeki hidrojen miktarını önemli derecede etkilediği tek faktör için yapılan varyans analizi ile anlaşılmıştır. Ayrıca sıvı metal sıcaklığı ile sahip olduğu hidrojen miktarı arasındaki ilişki grafiksel bir yöntemle belirlenmiştir.

TABLE OF CONTENTS

LIST OF FIGURES

LIST OF TABLES

CHAPTER 1

INTRODUCTION

The use of aluminum castings in the automotive industry has increased incredibly over the past two decades. The driving force for this increased use is vehicle weight reduction for improved performance, particularly fuel efficiency. In many cases, the mechanical properties of the cast aluminum parts are superior to those of the cast iron or wrought steel parts being replaced.

For the production of aluminum alloy wheel, Al-Si casting alloys are mostly used as the raw material. Because of their good casting properties, this type of alloys provides the alloy wheel to have good corrosion resistance and strength so that the vehicle can adapt to the road and weather conditions.

The most outstanding criteria are the amount of alloying additions and their effects on the Al-Si casting alloys in order to decide that which type of Al-Si alloy ought to be selected as a right application for the relevant product. The main alloying elements of Al-Si castings are silicon, magnesium, iron, manganese, beryllium, zinc, strontium and titanium. Each element gives some special features to the casting alloy so that the alloy can be produced with desired properties. The compositions of these elements affect the final properties.

Aluminum casting alloy wheels are generally produced using low-pressure die-casting. For the application of this casting method, Al-Si casting alloys should be chosen owing to their high adaptation capability to the permanent metal molds. By the help of alloying elements, it is possible to achieve effective and efficient aluminum alloy wheel production. Aluminum alloy wheels have important advantages compared to the steel wheels. These advantages provide aluminum alloy wheel to be popular. However, in production of wheels, defects in the cast microstructure undermine performance characteristics.

There are different kinds of defects occur on Al-Si casting alloys. One of the most important of these defects is microporosity that can limit elongation and fatigue properties. The reasons of the defects can be related to the process features or mould specifications. Also, to minimize the concentration of defects, there are some remedies for each defect type. By applying these solutions, the defects are eliminated from the

material. For aluminum alloy wheel, realizing some corrections, such as changing the mold specifications, increasing casting temperature or changing the injection time of molten metal into mold can also decrease the casting defects. It is obvious that the important point is to know what should be done for each type of defect.

Quality improvement of aluminum alloy wheel production facilitates understanding the process parameters and their influences on the defect formation. To decrease the amount of scrap and rework, satisfactory quality of the production has to be achieved. This can be done using quality improvement tools. This work enables the management to get information about the production status and the role of parameters during production. As a result of this, it is possible to reach some remedies for achieving high quality performance.

Controlling process parameters can decrease defects on aluminum alloy wheel and the amount of scrap produced. In this study, defects on aluminum alloy wheel were investigated by means of real time radioscopic method. The production parameters of defected wheels have been recorded.

In present study, quality improvement of cast Al wheel production has been investigated in three aspects, production line, defects and the role of hydrogen content and density index on gas hole formation. In each group, the reasons of affecting the quality have been investigated and the remedies have been proposed.

In order to supply ease of presentation of current study and discussion of the results; in Chapter 2, theoretical background and up-to-date review of widespread applications are presented, giving aluminum alloy wheel production, defects on Al-Si cast wheels, quality control, quality improvements of the process and quality improvement tools. The essential of experimental procedure of quality improvement of Al-wheel production is presented in Chapter 3. Reasons of experiments and discussion are provided in Chapter 4.

CHAPTER 2

THEORY AND LITERATURE SURVEY

2.1. Al-Si Casting Alloys

Aluminum cast alloys have been developed for casting qualities such as fluidity and feeding ability, as well as for properties such as strength, ductility, and corrosion resistance. Thus, their chemical compositions differ widely from those of the wrought aluminum alloys [1].

Because pure aluminum is a relatively poor casting material, aluminum casting is actually made of an aluminum alloy. Since there are over 100 aluminum-based casting alloys, it is evident that quite different properties may be obtained from the various alloys. For these alloys there are two types of properties that should be considered. There are the casting properties, those characteristics of the alloy, which determine the ease or difficulty of producing acceptable castings. Then, there are the engineering properties that are those properties of interest to the designer or user of the castings [2]. The most important aluminum casting alloys are [1,3,4] aluminum- copper, aluminum-silicon, aluminum-zinc and aluminum-magnesium casting alloys.

Aluminum casting alloys with silicon as the major alloying element are the most important commercial casting alloys because of their superior casting characteristics. Aluminum-silicon alloys have comparatively high fluidity in the molten state, excellent feeding during solidification, and comparative freedom from hot shortness. Silicon does not reduce the good corrosion resistance of pure aluminum, and in some cases increases its corrosion resistance in mild acidic environments [1].

Yakhtin et al. [5] studied Al-Si alloy system. These alloys are also called “silumin alloys”. One of the disadvantages of the silumin as a casting alloy is the porosity of the castings often obtained. The addition of magnesium and copper, which forms the compounds Mg_2Si and $CuAl_2$, enables silumin alloys to be heat-treated.

The applications of aluminum-silicon casting alloy products are numerous and quite varied. Some of the most important application fields of Al-Si casting alloys are given in Table 2.1.

Table 2.1. Typical applications of the Al-Si alloy [6]

Alloy Type	Application
-A380.0	Bracket housings, internal engine parts
383.0	Blocks, transmission housing-parts, fuel metering devices
319.0	Manifolds, cylinder heads, blocks, internal engine parts
356.0	Cylinder heads, manifolds
-A356.0	Wheels
-B390.0	High wear applications such as ring gears and internal transmission parts

2.1.1. Effects of Alloying Additions on the Properties of Al-Si Casting Alloys

Shibata et al. [7] studied on high toughness and high strength aluminum alloy casting. They developed some standard values for alloying additions and discussed the effects of these additions.

As far as an aluminum casting used as strength-requiring member for an automobile, like, as a wheel, both strength and safety are important, in addition, excellent mechanical properties such as soundness, toughness, in particular high elongation, high yield and tensile strength are required.

Effects of alloying additions are given in [4,7,8]:

Si (Silicon) determines the castability of the alloy. When Si content of the alloy is less than 4%, the castability is poor with considerable shrinkage cavities accompanied. Silicon contents from about 4% to the eutectic level of about 12% reduce scrap losses, permit production of much more complex designs with greater variations in section thickness and yield castings with higher surface and quality. These benefits derive from the effects of silicon in increasing fluidity, reducing cracking and improving feeding to minimize shrinkage porosity.

Mg (Magnesium) is typically incorporated to enhance the tensile strength of the alloy. However, while increased magnesium content enhances the hardness and fatigue resistance of the alloy, it also decreases the alloy's ductility. An additional reason for limiting magnesium content in the alloy is that magnesium can easily form MgO

microsized particles in the melt. These oxides can form rapidly forming inclusions in the melt. These inclusions reduce the fluidity and the ductility of Al-Si casting alloys.

The effects of alloying additions on tensile strength and ductility are shown in Figure 2.1.

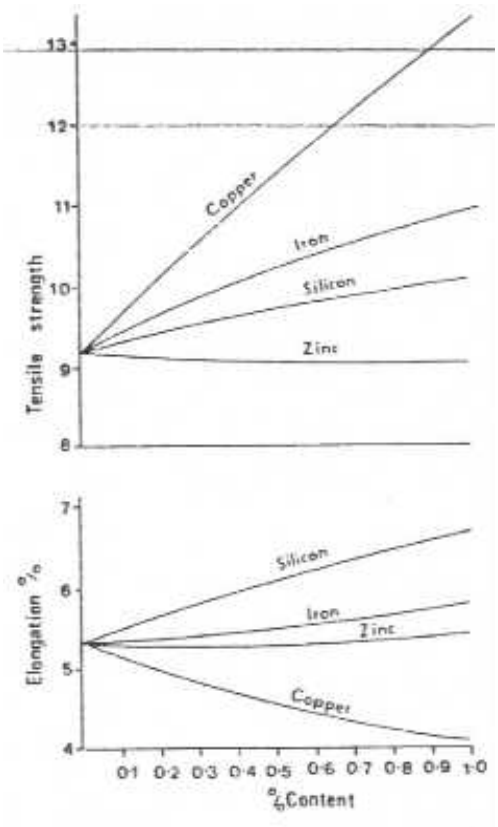

Figure 2.1. Effects of alloying additions on tensile strength and ductility [3]

Fe (Iron) is known as an element impairing the toughness of resulting casting. It is typically added to die cast Al-Si alloys for the purpose of preventing the aluminum alloy from sticking to the metal die during the casting process and enhancing the release of aluminum alloy from the die.

Mn (Manganese) is added to a compound containing Fe to permit said crystallized compound to have some slight roundness. It is also added to eliminate the adverse effect of the iron-addition. However, an excess amount of manganese can result reduction in mechanical strength.

Cu (Copper) can also be added to Al-Si alloy to increase the strength of the alloy. As copper content increases, hardness of the alloy increases. The strength and ductility depend on whether the Cu is in solid solution or not and homogeneous distribution of particles. Also, copper decreases electrolytic potential and the corrosion resistance.

Be (Beryllium) is included in Al-Si casting alloys to enhance the corrosion resistance, elongation and strength of Al-Si alloys. Evans et al. [8] found that the mechanical properties of Al-Si alloy can be enhanced by lowering Be content below 0.003% by weight.

Zn (Zinc) addition promotes hot shortness and it has poor stress corrosion resistance.

Ti (Titanium) addition increases the corrosion resistance of the alloy. It is generally added as AlTiB in order to provide the grain refinement of aluminum. The optimum grain refiner addition has to be component specific, and depends on the complexity of the casting as well as the casting method applied.

Sr (Strontium) addition to the melt provides the modification on castings having a content of 5-13% Si. This addition changes the Si particles in the solidified material from a plate-like or acicular shape to a fibrous phase.

By modifying Al-Si castings, mechanical properties are improved, particularly with regard to the elongation and fracture toughness. Most pronounced is the improvement on large castings having thick sections.

The most important low-pressure permanent mold casting Al-Si alloys and their chemical compositions are summarized in Table 2.2.

Table 2.2. Chemical composition limits of LPPM Al-Si casting alloys [9]

Element	319.0	333.0	354.0	356.0	A356.0	357.0
Silicon	5.5-6.5	8.0-10.0	8.6-9.4	6.5-7.5	6.5-7.5	6.5-7.5
Iron	1.0	1.0	0.2	0.6	0.2	0.15
Copper	3.0-4.0	3.0-4.0	1.6-2.0	0.25	0.2	0.05
Manganese	0.50	0.50	0.10	0.354	0.10	0.03
Magnesium	0.10	.50	.40-.60	.20	.25-.45	.45-.60
Chromium	0.00	0.00	0.00	0.00	0.00	0.00
Nickel	0.35	0.50	0.00	0.00	0.00	0.00
Zinc	1.00	1.00	0.10	0.35	0.10	0.05
Titanium	0.25	0.25	0.20	0.25	0.20	0.20
All others	0.50	0.50	0.20	0.20	0.20	0.20
Aluminum	Remainder	Remainder	Remainder	Remainder	Remainder	Remainder

2.2. Aluminum Alloy Wheels

Wheel is a component that supports tire. This name is also usually called instead of “rim”. Generally, there are two main types of wheels are manufactured for the vehicles like steel and aluminum alloy. Aluminum alloy wheel is the second most popular wheel after steel one [10,11].

The advantages of Al alloy wheel are [12,13]:

- Highly styling versatility
- Any size available
- Unique style
- Weight savings
- Minimum trim
- Best wheel uniformity
- Various “bright look” options
- Low tooling costs

The advantages of Al alloy wheels over the steel wheels are [11];

1. They provide less fuel consumption. Because density of Al is only 1/3 of the steel. And for 4-aluminum wheels/car, the total weight reduction is 4-8 kg. Consequently, the fuel saving rate is about 7%.

2. Al wheels have better performance than steel wheels. Because of lighter weight, Al wheels gain more quick acceleration and short braking distance.

3. With Al wheels, driving is more comfortable. It means to get excellent impact absorption and more accurate balancing.

4. Al wheel utilization maintains effective dissipation of heat. It improves the service life.

5. By using Al wheels, there becomes no air leakage. Because of precise and accurate machine usage, there occurs very rare air leakage and excellent safety.

6. Al alloys wheels have good corrosion resistance. They are suitable for running under very severe weather conditions.

7. Al alloy wheels have outstanding appearance. Actually, they have various style and brightly shining surface. They are also very attractive.

After passing some developments, Al alloy wheels has jumped to the highest point in the industrial sector. In the middle of 1920s, one piece of Al alloy wheel has been developed. About 20 years later, in the late of 1940s, the forged Al wheel became popular at that time. At the end of 1960s, the Al alloy wheels completed their main development with the invention of multi-piece Al alloy wheels [11].

2.2.1. The General Types of Al Alloy Wheels

The types of Al alloy wheels are given in [12,13] and they are,

1. Forged Al Alloy Wheels
2. Single piece Al Alloy Wheels
3. Multi piece Al Alloy Wheels

Forged Al alloy wheels are generally used in medium and heavy trucks. A forged Al wheel is shown in Figure 2.2. Forged wheels are manufactured by using one piece of aluminum alloy that gives fuel savings, greater payloads and lower weight.

Most Al wheels are single-piece castings manufactured from a variety of casting processes (Fig. 2.3.). The cast product provides an infinite number of styling iterations and optimized for minimum weight and cost. This type of wheels can be used in passenger cars, minivans, sport utility vehicles and etc.

Figure 2.2. Forged Al alloy wheel [12]

Figure 2.3. Single piece Al alloy wheel [13]

Multi piece wheels are actually manufactured from two or more components that are securely welded together. The process has the unique advantage of having a rolled-and-spun wrought aluminum rim combined with a cast disc, made of mold (Fig. 2.4.). This cast disc can provide lower tooling cost.

Figure 2.4. Multi piece Al alloy wheel [13]

2.2.2. General Structure of Aluminum Casting Alloy Wheel

Al cast alloy wheel includes an aluminum body part and a cover as a design part, which is removable, fitted to the aluminum body part. The cover body of Al wheel is shown in Figure 2.5. and also the body part is shown in Figure 2.6.

Kato et al. [14] studied on Al casting alloy wheels and some conclusions were given. The aluminum body part, including a rim part and disc part, imparts a desired strength to the wheel. The cover has substantially disc-shaped cover body that covers a front face of the aluminum part, and fixing means, arranged circumferentially with a spacing there between, which is installed on a rear surface of the cover body.

For an aluminum wheel, there are mainly three critical regions. These regions are [14] given in Figure 2.6. as:

- Rim flange portion (numbered as 3)
- Spokes (numbered as 6)
- Mounting parts (numbered as 5)
- Hub (numbered as 2)

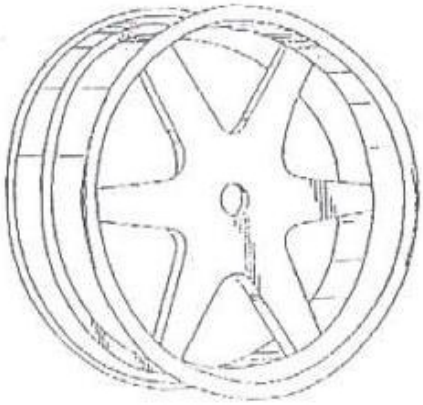

Figure 2.5. The cover body of Al wheel [14]

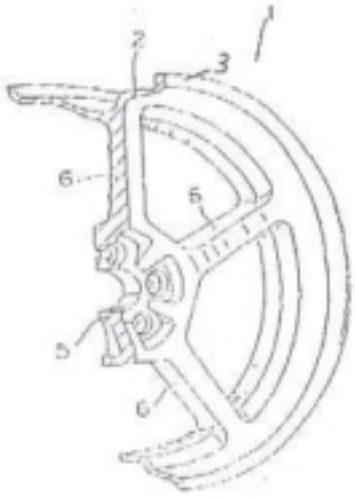

Figure 2.6. The body part of Al wheel [14]

2.3. Aluminum Alloy Wheel Production

During the manufacturing of Al wheels, casting methods can be used. These general methods are gravity casting, low-pressure die casting, high-pressure die-casting and squeeze casting as listed in Table 2.3.

The most important casting method is low-pressure die-casting. Because of its many advantages, single piece types Al alloy casting wheels are manufactured by using low-pressure die-casting.

The main advantages of low-pressure die-casting are given as [11]:

- Design versatility
- High productivity
- High dimensional accuracy
- Good surface quality
- Good mechanical strength
- Low equipment & dies cost
- The most popular & economic method

Al wheel production involves with several production steps. These steps are [3,4,11,15]:

a. Melting of Al Alloy

b. Degassing Process

c. Low Pressure Die Casting

d. Solidification of Al Alloy

e. Real Time Radioscopic Inspection

Table 2.3. Comparison of casting methods [16]

	Plaster casting	**Sand casting**	**Shell mould casting**	**Gravity die casting**	**Low pressure die casting**	**Pressure die casting**
Weight of the casting, kg	0.1...25	0.1...150	0.01...20	0.01...50	1...70	0.01...30
Annual volume	1...500	1...5000	500...10 000	100...50 000	100...10 000	1000...1 000 000
Pattern/tooling cost	Low/moderate	Relatively low	Relat low/moderate	Moderate	Moderate	High
Cost of changes	Relat.low/ moderate	Low	Relat.low/ moderate	Moderate	Moderate	High
Flexibility of design	High	Very high	High	High	Relatively high	Relatively high
Minimum wall thickness, mm	1...3	4...6	2...4	2...3	3...4	0.8...1.5
Dimension accuracy	Good	Fairly good	Good	Good	Good	Very good
Possible surface roughness, Ra	≥2.5(1.6)	≥6.3	≥3.2	≥3.2(2.5)	≥3.2	≥1.6(0.8)
Casting alloys	GS-AlSi12 GS-AlSi10 Mg GS-AlSi7 Mg	GS-AlSi12 GS-AlSi10 Mg GS-AlSi7 Mg	GS-AlSi12 GS-AlSi10 Mg GS-AlSi7 Mg	GK-AlSi12 GK-AlSi10 Mg GK-AlSi7 Mg	GK-AlSi12 GK-AlSi10 Mg	GD-AlSi8Cu3Fe GD-AlSi12 GD-AlSi10Mg GD-AZ91HP(Mg) GD-ZnAl4Cu1 (Zn)
Special features	Also with sand cores	Also heat-treated	Also with sand cores and heat-treated	Also with sand cores and heat-treated	Also heat-treated	Not heat-treatable

There are several steps during the production of aluminum casting alloy wheel. Figure 2.7. shows the process flow diagram of cast Al wheel production. In the beginning of the production, the ingots are melted in the furnace. Then, molten metal is transferred to holding unit and as a second step, degassing process is applied to the molten metal. After degassing, the metal is ready for die-casting. At this step, under low pressure alloy wheel is shaped and then it solidified. Finally, wheels are inspected by real time radioscopic inspection unit for achieving quality control. If the defects on the wheel are within the standards, it is accepted. Otherwise, it is sent to the melting unit to be added to the molten metal as a scrap. Also, leakage, impact and fatigue tests can be applied for some produced wheels as other types of quality control step.

Degassing of the molten alloy is an important step. Because, this process helps to reduce the amount of hydrogen gas that is dissolved in the metal. And, hydrogen gas is the most important reason of defect occurrence in the aluminum casting alloy wheels. As a result of this, it is necessary to take care of degassing process.

2.3.1. Melting of Al Alloy

Melting of Al alloy for die-casting entails three different types of operations [4]:

a. Melting down of virgin ingot

b. Remelting of scrap from the foundry and from trimming operations and reconstitution of this melt by means of suitable additions.

c. Holding of quantities of molten metal at a closely controlled temperature.

For the melting process, reverberatory furnaces and electric furnaces are used [4,11,17]. After melting process, molten metal generally has two transfer operations. Firstly, molten metal is transferred from melting furnace to holding furnace. And then, it is again transferred from holding furnace to the shot chamber of the die casting machine. Metal should be transferred at, or above, the holding temperature. When this is done, wide fluctuations in metal temperature are avoided. The schematic diagram of shaft melting furnace is given in Figure 2.8.

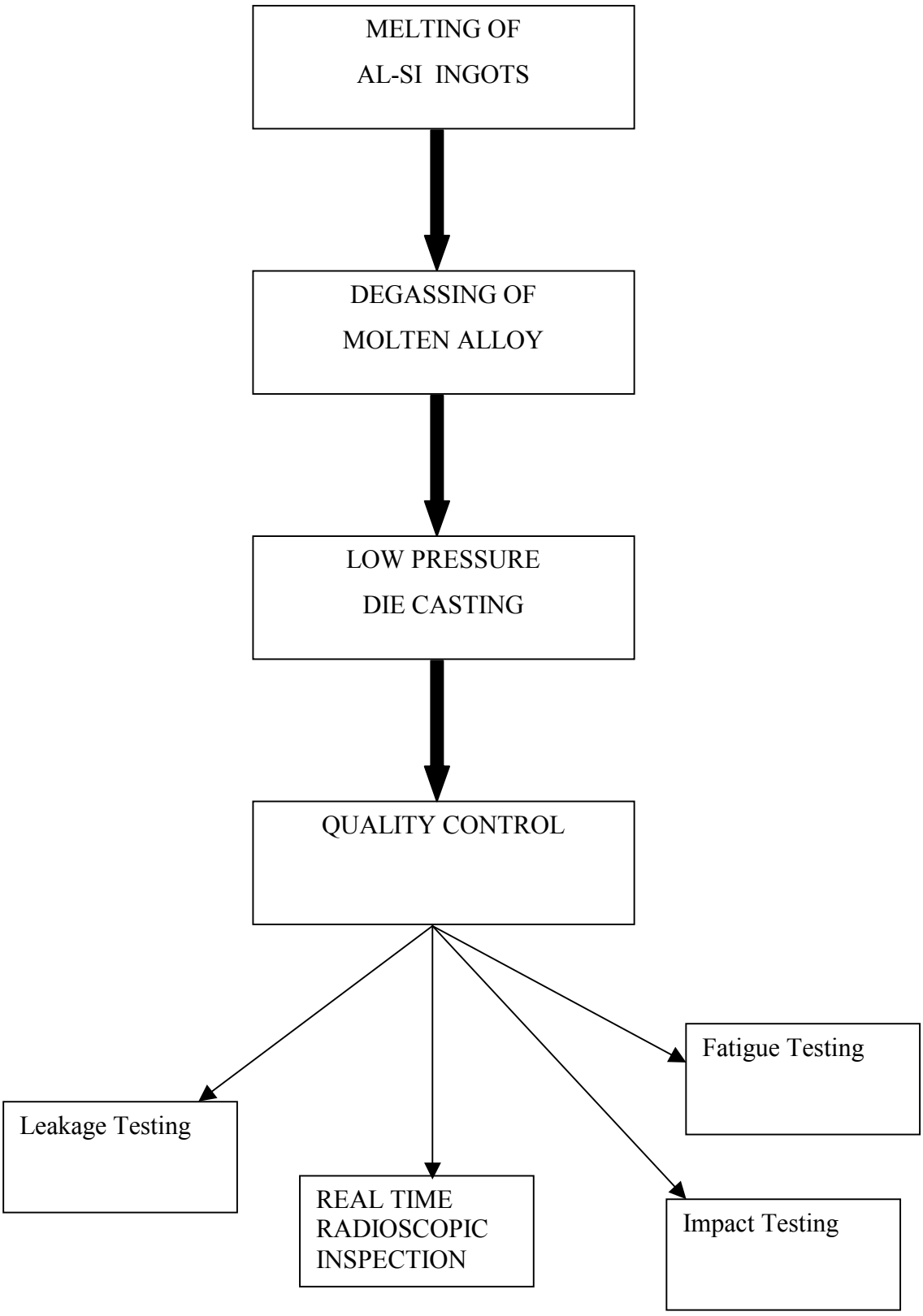

Figure 2.7. Process flow diagram of Al wheel production

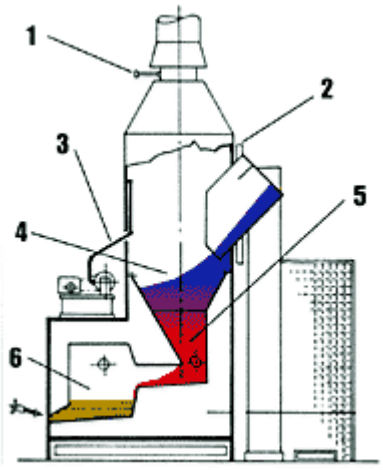

1. Exhaust gas control
2. Ingot loading gate
3. Confidence zone
4. Pre-heating zone
5. Melting zone
6. Holding unit

Figure 2.8. Schematic diagram of shaft melting furnace [18]

2.3.1.1. Hydrogen in Aluminum Alloys

It is generally recognized that H_2 is the only gas dissolves in molten metal. When two atoms combine to form a molecule, the gas escapes but still may be trapped as bubbles.

Little hydrogen is absorbed from the negligible amount of free hydrogen in the atmosphere. The main sources of hydrogen are water vapor and steam. Water vapor is the most common source and is 9% hydrogen by weight. One of the most likely sources of water vapor is the furnace combustion atmosphere, which contains about 18% water vapor. Nascent or atomic hydrogen, which is very active and quickly absorbed by molten aluminum, is produced by the chemical reaction:

$$3H_20 + 2Al \longrightarrow 6H + Al_2O_3 \qquad (2.1)$$

Sources of hydrogen porosity are:

-The furnace atmosphere, which contains appreciable amounts of water vapor in addition to some hydrogen;

-Moisture from refractories, dirty skimmers and furnace tools;

-Hydrated corrosion products that form part of the charge, such as weathered ingot and scrap;

-Oil-contaminated turnings, chips or scrap;

-Damp fluxes;

-Oil and hydroxide coating on metallic sodium used for modifying aluminum-silicon alloys.

The temperature of the molten metal determines amount of hydrogen absorbed. As the temperature rises, the volume of hydrogen taken into solution increases rapidly as shown in Figure 2.9. Solubility in the solid metal is practically nil; however, it jumps from a very small measurable quantity at just below the melting point to over 0.7cc/100g when the metal is molten at a little above the melting point. Alloys with a hydrogen content of less than about 0.01cc/100g remain practically free of gas pores and blisters.

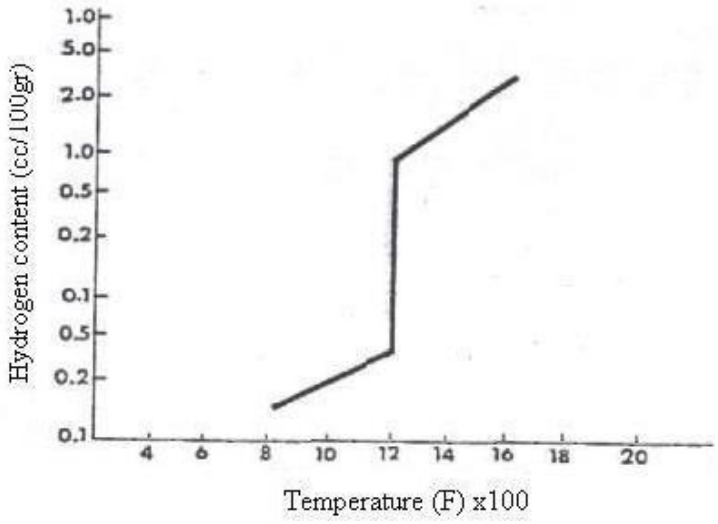

Figure 2.9. Hydrogen solubility curve due to temperature in aluminum [19]

A skin of aluminum oxide forms on the surface of molten aluminum in contact with air. Hydrogen trapped in this skin will produce porosity in castings if mixed in with the melt during turbulent pouring.

2.3.1.2. Measuring Hydrogen Concentration

The measuring of hydrogen in molten alloys allows the foundry to assess the melt quality before the casting operation. There are several methods available to the foundryman to assess the hydrogen concentration. These methods are;

-Reduced Pressure Test (Straube-Pfeiffer Test)

-Quantitative Reduced Pressure Test (Severn Science)

-Density Measurements

-Initial Bubble Test (Hycon Test)

-Recirculating Gas Test (Telgas, Alscan)

Reduced Pressure Test (Straube-Pfeiffer) is commonly used to assess hydrogen content of a melt. The test consists of solidifying a sample under reduced pressure (usually 1-100mm Hg). Gas pores that form are molecular and obey the gas law; therefore, they expand because of the reduced pressure and produce larger pores if the sample is allowed to solidify under atmospheric pressure.

Reduced pressure testers are at relatively low cost. The tester consists of a vacuum pump connected to a bell jar with a vacuum seal. Molten aluminum is placed in a small, preheated crucible on an insulated pad and covered with the bell. A vacuum is then applied to the bell.

Relatively small quantities of gas can be detected. If the melt contains a large quantity of gas, the sample will swell; if gas-free, it will normally sink. The solid slug can then be sectioned to check for relative gas content.

RPT is most effective if the sampling is done in a repeatable sequence that eliminates or reduces variables. Care should be taken to keep testing conditions (e.g. the pressure and the solidification rate/temperature) the same from test to test to avoid inconsistent results.

Quantitative Reduced Pressure Test (Severn Science) includes with allowing a constant amount of metal to solidify in a vacuum chamber. Hydrogen gas is evolved as the solidification proceeds and raises the pressure in the chamber. The amount of hydrogen is calculated from the pressure rise and displayed on a digital readout. Sensitivity is good at high hydrogen concentrations, but difficulties are experienced with concentrations of less than 0.1cc/100g Al.

Density Measurements is the simple way of indirectly measuring the hydrogen content of the melt. A sample is cast and the density is measured by weighing the sample in air and water (Archimedes Principle) using,

$$D_S = W_A/(W_A-W_W) \quad (2.2)$$

where, D_S is the density of sample, W_A is the weight of the sample in air and W_W is weight in water. The volume of hydrogen can then be determined by

$$H_2 = 1/(D_S-D_T) \quad (2.3)$$

where, D_T is theoretical density of the alloy, which can be determined by the alloy chemistry or by measuring the density of a sample that has been thoroughly degassed and chilled.

This technique is based on the assumption that all internal porosity is due to hydrogen. If the porosity is due to gas and shrinkage, the amount of hydrogen will be

overestimated. Because pores will form on solid inclusions, filtered metal is denser than unfiltered metal at the same hydrogen content. Differences between D_S and D_T are extremely small, so detecting these differences require precise instrumentation. Hydrogen concentration can, therefore, be calculated more easily for samples solidified under vacuum using a suitable correction factor.

Initial Bubble Test (Hycon Test): The pressure over a molten metal sample in a closed chamber is slowly reduced. When the first bubble of hydrogen breaks the surface, the pressure and temperature are recorded. The pressure equals the partial pressure of hydrogen in the melt. Knowing the temperature, hydrogen content can be determined based on Sievert's Law:

$$\underline{H} = k.(pH_2)^{(1/2)} \tag{2.4}$$

where, $\underline{H}$ is hydrogen concentration, pH_2 is the partial pressure of hydrogen in the surrounding atmosphere and k is a temperature-dependent constant.

Recirculating Gas Test (Telgas, Alscan) measures for hydrogen content directly. A small volume of nitrogen is recirculated through the molten bath. As the nitrogen circulates through the bath, it picks up hydrogen and eventually the hydrogen in the nitrogen and in the bath reaches equilibrium. The partial pressure of the hydrogen in the nitrogen equals to the partial pressure of the hydrogen in the molten bath. The hydrogen content is determined by measuring the thermal conductivity of the hydrogen-nitrogen mixture [20].

2.3.1.3. Solubility of Hydrogen Gas

Sievert's Law (2.4) [21] states that the amount of gas dissolved in the melt varies with the square root of the partial pressure of the gas in the atmosphere over the melt and is given in the following equation as,

$$\%[H]=K.\ (P_{Hydrogen})^{1/2} \tag{2.5}$$

K value can be evaluated from the data for one atmosphere of pressure.

If the pressure is maintained constant, the solubility of a gas with temperature e.g. hydrogen can be expressed by the Van't Hoff equation; where $\Delta H°$ is standard enthalpy, and $\underline{H}$ is the hydrogen solubility.

$$\frac{\partial}{\partial T}(\ln K)_p = \frac{\Delta H^0}{RT^2} = \frac{2\partial}{\partial T}\ln \underline{H} \tag{2.6}$$

If $\Delta H°$ is taken constant over a small range of temperatures, integration of equation (2.6) gives:

$$\ln \underline{H} = \frac{\Delta H°}{2RT} + \text{constant} \qquad (2.7)$$

If $\Delta H°$ is positive, the reaction will be endothermic and therefore, $\underline{H}$ will increase with temperature. This is normal case in metallic systems. The solubility of gas is generally expressed as cm^3 of gas per 100g of solution. For hydrogen in liquid Al the relationship can be given as,

$$\log(C/\underline{C}) = -2761/(T/K) + 2.768 \qquad (2.8)$$

For the solid, the relationship is given as,

$$\log (C/\underline{C}) = -2580/(T/K) + 1.399 \qquad (2.9)$$

where, C is the dissolved gas concentration and $\underline{C}$ is a standard unit defined as $1cm^3$ of hydrogen at 273K and 1atm. per 100g melt [22].

2.3.2. Degassing

Before the beginning of die casting, the molten metal taken from the holding unit, should go into "degassing process". The gas, employed for a degassing operation of an aluminum melt, may be inert to Al, as argon, helium or nitrogen, or a gas like chlorine which can react.

For an inert gas, the removal of hydrogen from the melt is dependent on the reaction at the melt-gas bubble interface:

$$2\underline{H} \rightleftharpoons H_2 \text{ (gas bubble)}$$

$$\underline{H}^2 = K_1 \, pH_2 \qquad (2.10)$$

where $\underline{H}$ is the hydrogen concentration, K_1 is temperature dependent constant and pH_2 is the partial pressure of hydrogen in the surrounding atmosphere. For a freshly formed bubble in which $pH_2 = 0$, hydrogen gas transfer from the metal to the bubble at the interface according to the relationship given in Equation (2.10). Each bubble takes with it a part of the dissolved hydrogen and the volume of gas required could be calculated from the equation as follows:

$$V = K\left[(C^{\Theta})^2\left(\frac{1}{C_F} - \frac{1}{C_I}\right) + (C_F.C_I)\right] \qquad (2.11)$$

where, C_F is the final hydrogen content, C_I is the initial hydrogen content, C^{Θ} is the solubility of hydrogen in the melt for standard hydrogen pressure and K is a constant depending on the mass of the metal. Then, the volume of the gas passed is a function of C^{Θ}, the initial concentration of hydrogen and final concentration to be attained. C^{Θ} is dependent on the temperature and therefore, degassing is made at the lowest temperature possible. Since equilibrium is not attained, degassing is less efficient than that of given in Equation (2.11).

This model was modified to allow for the kinetics of mass transfer. The modified model is well fitted to the practical degassing [22]. Practically, all methods for hydrogen removal center about Sievert's Law i.e., they seek to reduce the partial pressure of hydrogen over the melt. For degassing process, three corrective steps can be applied [4,21,23]:

1. Molten metal temperature is reduced, before castings are poured.

2. The ratio of air to oil in the melting furnace is changed to provide oxidizing flames, thus reducing the possibility of hydrogen pick up from this source.

3. The metal is degassed with a mixture of nitrogen, chlorine, helium or argon.

These steps are all effective in eliminating porosity. A schematic diagram for degassing process is given in Figure 2.10. In this degassing method, an inertgas, preferably Argon is injected into the flow of molten Al-Si alloy through one or two piece injection nozzles. A dry insoluble gas such as chlorine, nitrogen, argon or nitrogen is bubbled through the melt. The hydrogen diffuses into the bubbles in an amount that satisfies the equation (2.8). In this way, the amount of hydrogen is gradually reduced [19,24,25].

For many years, chlorine and nitrogen have been the most common degassers for molten aluminum. The gas is bubbled through molten aluminum to remove absorbed hydrogen. The bubbling action also helps oxide particles to float to the surface. In this sense, chlorine and nitrogen can be classed as cleaning fluxes.

The use of straight chlorine has been greatly reduced and replaced by use of mixtures of 10% chlorine-90% nitrogen or 10% chlorine-90% argon. Also, fluxing with 100% nitrogen or 100% argon becomes more popular [20].

The spinning action of the nozzle creates a large number of small gas bubbles that are mixed with the liquid alloy. With the addition of low percentage of chlorine (less than 0.5% of the process gas flow) non-wetted inclusions will attach themselves to the rising bubbles and will be removed from the melt. The addition of chlorine will also

reduce the concentrations of alkali metals (Na, Ca, Li and K) to form their respective chloride salts.

Degassing fluxes to remove hydrogen are recommended after the surface of the bath has been fluxed for removal of oxides. The degassing fluxes also help to lift fine oxides and particles to the top of the bath. Fluxes and refining agents are generally applied for the removal of alkali metals and nonmetallic inclusions from Al-Si molten alloy [4,24,25].

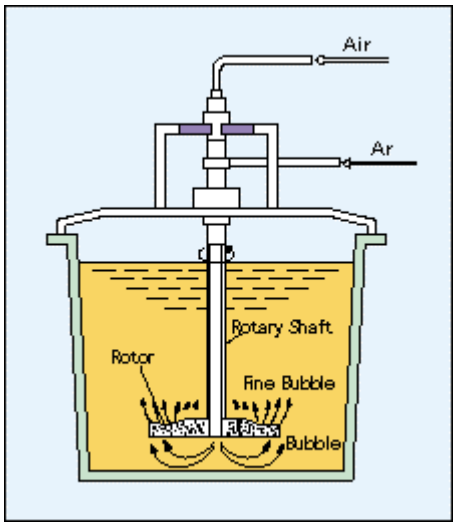

Figure 2.10. Schematic diagram of degassing process [4]

2.3.3. Low Pressure Die Casting

Forcing molten metal under pressure into permanent steel dies produces die-castings. Die-casting involves metal flow at high velocities induced by the application of pressure. Because of this high-velocity filling, die-casting can produce shapes that are more complex than shapes that can be produced by permanent mold castings [4,17,26].

By using low-pressure die-casting, relatively complex shapes can be produced. Production rates are higher and metal cost is often lower than those of other casting processes. High dimensional accuracy can be achieved without significant alterations [27,28].

In Al wheel production, vertical low-pressure die casting principles are applied, schematic diagram is given in Figure 2.11. In this process, molten metal is introduced into a die from below by means of the low-pressure gas applied to the metal in a sealed furnace.

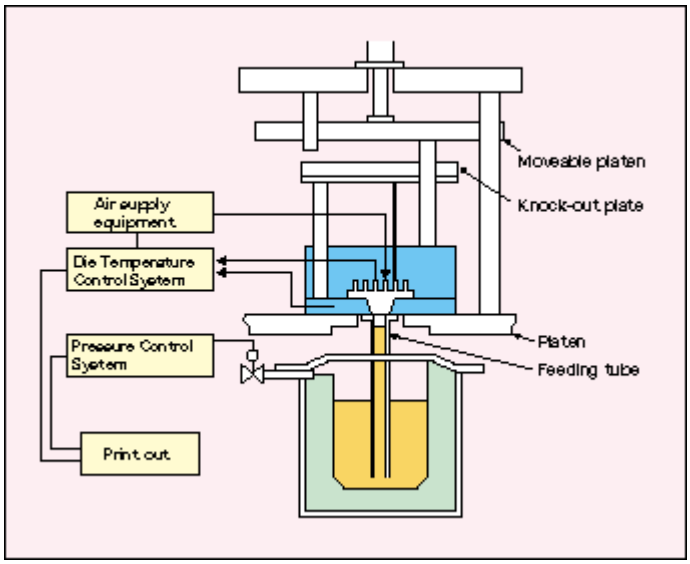

Figure 2.11. Schematic diagram of a vertical low pressure die casting machine [4]

As it can easily be seen in Figure 2.11., metal is injected from below of the die. Air is evacuated from the die and molten metal is drawn into the shot chamber by vacuum. Pressures for clamping the dies and injecting the metal are controlled by a single accumulator source, which maintains a balanced pressure even in the event of a malfunction. The die casting machine is located over a water-filled tank that is fitted with a conveyor for transporting the castings to the next operation with the cooling operation [4,29].

Die casting dies are basically similar to heat exchangers and optimum die temperature for a specific casting is determined by section thickness and by the type of finish required. When optimum die temperature has been established, it should be maintained within ±6°C. For casting Al alloys, such as AlSi, the usual range of die temperature is 220 to 315°C, with the average near 290°C [4].

Die lubricants prevent adhering of the cast to the die and provide the casting with a better finish. A correctly chosen lubricant will allow metal to flow into cavities that otherwise can not be filled. The cycle time to produce a die-casting depends on the size and weight of the shot. These basic factors are interrelated with machine capability, die opening and closing time, pouring time, injection time, dwell time, metal temperature, time for die lubrication and time for application of lubricant [4,27,30,31].

2.3.4. Solidification of Al-Si Alloy

Al-Si casting alloys are required to have some properties. These properties include small dendrite size, low porosity and small grain size. Getting small grain size can be achieved by producing turbulence in the liquid using a low thermal conductive mould and adding grain refiners [32].

Al-Si is a simple eutectic system with two solid solution phases. There are three main groups of Al alloys, which contain silicon [3,33]:

1. Hypo-eutectic 2.0 – 7.0%
2. Eutectic 8.0 – 13.0%
3. Hyper-eutectic 16.0 – 25%

Al-Si phase diagram was given in Figure 2.12. and also in Table 2.4. , some special points of Al-Si alloy system are given.

Table 2.4. Special points of the Al-Si system [33]

Reaction	**Composition (weight %Si)**	**Temperature (˚C)**	**Reaction Type**
L ↔ Al	0	660	Melting
L ↔ (Al) + (Si)	12.6	577	Eutectic
L ↔ Si	100	1412	Melting

In Figure 2.12. , Guy gives the equilibrium diagram for Al-Si alloys, with photo micrographs showing the representative structures at room temperature. The photomicrograph of 99.95% aluminum exhibits the typical equiaxed grain structure of a pure metal. The microstructure of the 8% silicon alloy shows long dendrites of primary α-solid solution surrounded by the eutectic microconstituent. In contrast, when the primary solid phase is the silicon rich β phase (in the 20% and 50% silicon alloys), the primary phase crystals have geometric shapes.

Grain refinement in Al alloys are important in order to get a uniform solidification pattern and sound product. Grain refinement is obtained with the addition of Ti, Zr, V and joint addition of B and Ti. It is also determined that $TiAl_3$, VAl_{10}, $CrAl_7$, $NiAl_3$ and AlB_2 would be good nucleants for Al. By means of grain refinement, the rate of nucleation increases [34,35].

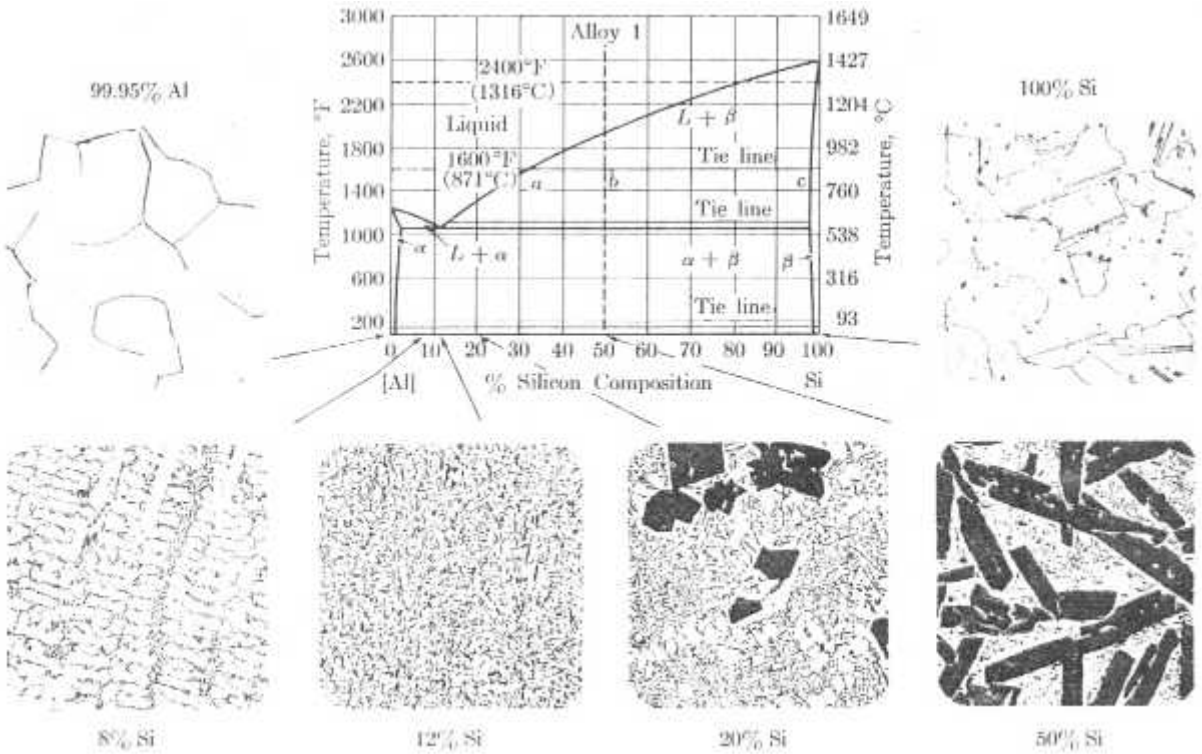

Figure 2.12. The Al-Si phase diagram and alloy system with some room-temperature microstructures [36]

2.4. Defects on Al Cast Wheels

The production of sound castings is of great economic importance. It is an essential step to be able to recognize the different kinds of defects that can arise in casting processes. Often errors in design can be overcome by the adoption of the procedures involving careful control of the cast metal and of the casting procedure. In many cases, in order to facilitate production it is of greater practical and economic merit to modify the design of an object to be cast [2,22,37].

Casting defects occur during the time that passes for the last solidification becomes, after the pouring of the molten metal into the mould, due to the different influences. Generally, defects can appear in different shapes, dimensions and visions due to the type of material, molding design, dimension of the specimen and process control and so like variables.

A casting defect can be either the function of only one cause or the result of many causes. Moreover, with the influences of the many causes, only one defect can occur [37]. The major defects that can occur in Al-Si alloys are given in Table 2.5.

Aygün [37] has found two groups of defects in Al-Si alloys based on Real-time Radioscopic Method:

1. Hole Type Defects
2. Crack Type Defects

2.4.1. Hole Type Defects

Blow Holes: In general, this type of defects can be easily inspected owing to having smooth surfaces with a spherical shape. Blow holes are round or elongated cavities, usually with smooth walls, found on or under the surface of the castings [2,22,37].

They can arise from a number of reasons [22]:

1. Because of the entrapment of the air during the pouring of metal into the mould.

2. Due to the reactions between molten metal with the mould or the core materials.

Table 2.5. Summary of Al-Si casting defects [22]

Defect	Cause	Foundry Remedy	Design Remedy
Blowholes	Occlusion of gases	1. Increased venting 2. Elimination of materials that can react to produce gas 3. Degassing	Avoid feed systems which have high flow velocities
Cold shuts	Non-union of metal streams	1. Raise pouring temperature 2. Preheat mould	Relocate runners and ingates
Contraction cracks	Tearing of the metal under thermal stress	1. Use collapsible moulds 2. Control of thermal gradients with chills	Avoid abrupt changes in section
Flash	Flow into the mould join	1. Lower pouring temperature 2. Increase mould box clamping	
Oxide and dross inclusions	Entrapment of foreign matter	Increase care and cleanliness during pouring	
Shrinkage cavities	Lack of sufficient feed metal	1. Promote directional solidification by control of heat flow 2. Raise pouring temperature	Relocate risers and ingates
Misruns	Low metal fluidity	Raise pouring temperature	Reconsider position, size and number of ingates and vents

3. As the result of chemical reactions taking place in the molten metal during cooling and solidification.

4. By the evaluation of gas during the solidification process.

These cavities can be small, when they are known as “pinholes” or of quite large size known as “gas holes”. Gas hole defect on an Al wheel is shown in Figure 2.13.

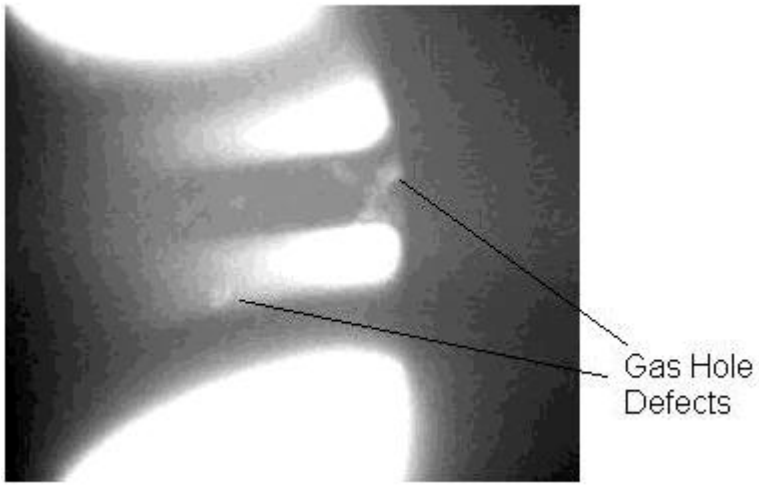

Figure 2.13. Gas hole defect in Al alloy cast wheel [38]

Most of the remedies for eliminating blowholes of type (1) and (2) involve changes in the practice. Care during pouring or the provision of extra venting will remove entrapped air, and prior to casting eliminates moisture, thus avoiding the evolution of steam.

If the cause is due to a chemical reaction, it is usually necessary to introduce additions into the metal to remove the reactants before gas is evolved.

Taking steps to eliminate the gas before the molten metal is introduced into the mould can only prevent the evolution of dissolved gasses. This can be done by degassing [22,37].

Porosity: One of the biggest problems in aluminum castings is porosity, caused mainly by 1) shrinkage resulting from the volume decrease accompanying solidification and 2) evaluation of dissolved gases, resulting from the decrease in solubility of these gases in the solid as compared to the liquid metal.

The condition for formation of a gas pore of radius r is:

$$P_g \geq P_0 + \rho_L gh + P_s + P_\sigma \quad (2.12)$$

where P_g is the gas pressure, P_0, $\rho_L gh$, P_s and P_σ are the ambient pressure, metallostatic pressure, shrinkage pressure and surface tension between gas and liquid, respectively. P_0 and $\rho_L gh$ are usually constants. P_g, P_s and P_σ need to be calculated from the mathematical model. Equation (2.12) shows that the gas pore can form only when the gas pressure is sufficiently large to overcome the total local external pressure [39].

Increasing the solidification velocity causes the pore radius to decrease and pore density to increase. Higher cooling rate reduces solidification time and grain size of the casting. Hence, grain density increases with cooling rate. The average pore size decreases with increasing cooling rate. With decreasing solidification time, there is less time for hydrogen to diffuse from the solidifying dendrite to the liquid. Hence, gas pore growth rate is inhibited [40, 41].

Porosity defect on an Al cast wheel is shown in Figure 2.14.

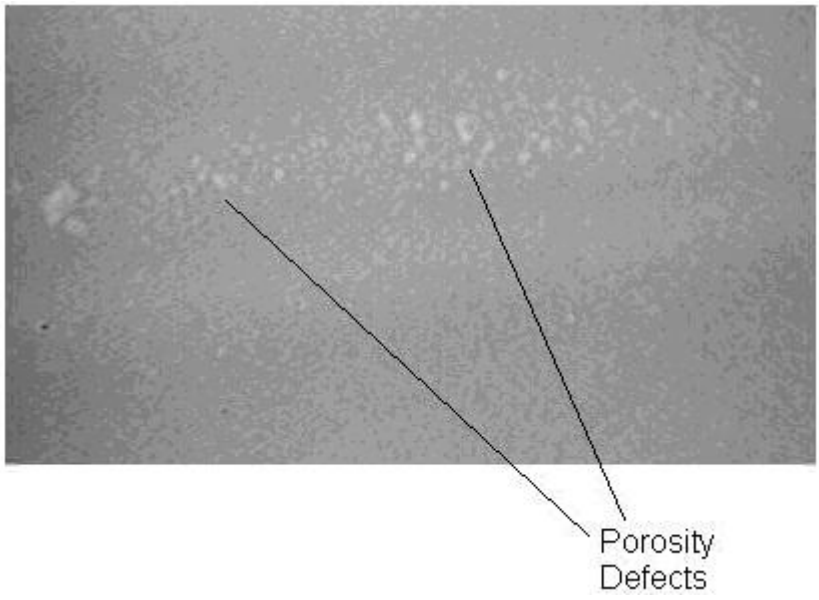

Figure 2.14. Porosity defect on Al alloy cast wheel [37]

Microporosity: This type of defect can be seen at the grain boundaries as in a territory shape and it is a very thin porosity.

The causes of this defect can be prevented, by decreasing the casting temperature, changing the design to eliminate the thick sections, decreasing the carbon equivalence, using chill and reducing the phosphorus content [2,37].

Oxide and Dross Inclusions: These result from the entrapment of surface oxide or other foreign matter during pouring. Often they are not immediately apparent and can only be clearly seen after machining of the casting surface. Insufficient skimming before pouring, the use of dirty ladles and turbulence due to improper grating methods can all contribute these defects. Redesign of the feed system and attention to care and cleanliness are needed to avoid these inclusions [22].

2.4.2. Crack Type Defects

Shrinkage Porosity: The majority of metals show a significant increase in volume on melting. This change in volume manifests itself as shrinkage during the reverse transformation from liquid to solid. If insufficient attention is given to ensuring that all parts of the casting are supplied with liquid metal throughout the whole of the solidification process, areas of liquid can become isolated. The shrinkage then appears as a cavity of irregular shape [22].

Typical shrinkage porosity on Al alloy cast wheel is shown in Figure 2.15.

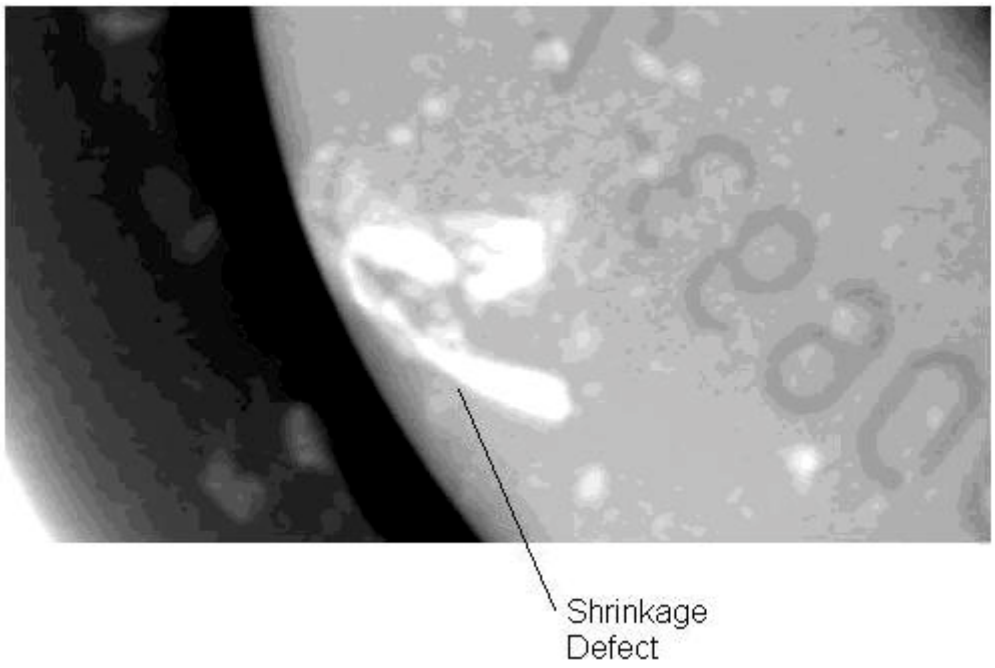

Figure 2.15. Shrinkage porosity on Al alloy cast wheel [37]

Micro Shrinkage: These are the branches shaped shrinkage holes between the grains and they are happened by the combination of many small shrinkage holes at the last solidified zone of the casting. By reducing the casting temperature modifying the design as eliminating the thick sections and using chill, the extent of these defects can be reduced.

Sponge Shrinkage: Sponge shrinkage is the area that is occurred the independent and irrelevant shrinkage holes. Sometimes, it is bigger than micro shrinkage and has a sponge shape. Generally, they occur on thin sections; on the thick sections, this defect occurs as a micro shrinkage.

Contraction Cracks: These are irregular shape cracks formed when the metal pulls itself apart while cooling in the mould or after removal from the mould.

When the crack appears during the last stages of solidification it is called “hot tear”. In this case, the crack faces are usually heavily oxidized. Hot tearing is the most common in metals and alloys that have a wide freezing range, and the isolated regions of liquid become subjected to thermal stresses during cooling and fracture results.

Several steps are necessary to avoid these defects. First, the cores and mould should be made more collapsible, for instance by incorporation of elastic soft material, e.g. cellulose, into the mould material or by minimizing the compaction during molding. In addition, alterations in design to avoid abrupt changes in section may be necessary. Hot spots can be eliminated, and thermal gradients controlled, by modification of the gating system or by the use of chills [22,37].

Cracks: Cold cracks appear during the application of a static load to the material that is over the maximum resistance of this metal.

In the corrosive situations because of the static load application, stressed corrosive cracks can occur. It happens in different parts of the material on where it was overloaded [37].

2.4.3. Other Casting Defects

Cold Shut: A cold shut is produced when two streams of metal flowing from different regions in the casting meet without union. The shuts appear as apparent cracks or wrinkles in the surface together with oxide films. This defect is usually the result of insufficient fluidity in the metal or the use of unsatisfactory methods of running and gating. Interrupted pouring can also give rise to cold shut formation. The remedy is to increase fluidity either by raising the pouring temperature or by preheating the mould. Relocation of runners and ingates can often be equally effective.

Misruns: An exaggerated form of shut is the misrun. These are produced when the liquid metal fails to fill the mould either because of low fluidity or if the methods of running are unsatisfactory. They are evident as smooth irregular-shaped holes, with rounded edges, through the casting wall. Poor venting of moulds and cores can have a contributory effect. Raising the pouring temperature and reconsidering the position, size and number of ingates and vents usually eliminate this defect.

Segregation: Al has small atom number and in Al alloys, some territories are richen by some alloy elements. Consequently, in these territories, concentration differences occur. Be got rich of a known element, generally occurs against to the center; it appears with the reaching of some elements which have a low melting point like as carbon, sulfur and phosphor to the center, along the solidification of these elements at here.

In some kinds of Al alloys inverse of this event forms. By heat input and using chill the homogenous distribution of alloy elements can be realized [22,37].

2.5. Quality Control

Quality has become one of the most important customer decision factors in the selection among competing products and services. The phenomenon is widespread, regardless of whether customer is an individual or an industrial program. Consequently, understanding and improving quality is a key factor leading to business success, growth and an enhanced competitive position [42].

The traditional definition of quality is based on the viewpoint that products and services must meet the requirements of those who use them. Quality can also be defined as fitness for use. There are two general aspects of fitness for use; quality of design and quality of conformance. Quality of design includes design differences, reliability obtained through engineering development of the product. The quality of conformance is how well the product conforms to the specifications required by the design [42].

Quality is inversely proportional to variability. If the variability decreases, the quality of the product increases.

The quality of a product can be evaluated in several ways. It is often very important to differentiate these different dimensions of quality.

Garvin [43] provided an excellent discussion of eight components or dimensions of quality as,

1. Performance

Will the product do the intended job?

2. Reliability

How often does the product fail?

3. Durability

How long does the product last?

4. Service ability

How easy is it to repair the product?

5. Aesthetics

What does the product look like?

6. Features

What does the product do?

7. Perceived Quality

What is the reputation of the company or its product?

8. Conformance to Standards

Is the product made exactly as the designer intended?

Generally, as quality control for Al wheel, there is some inspection methods, such as leakage testing, fatigue casting, impact testing and real time radioscopic inspection. But, the most outstanding method is the real time radioscopic inspection. Because, after the solidification of the casting, all produced wheels are inspected by RTR unit operator to understand whether the wheel will be accepted or rejected. The main aim of using RTR method for the inspection of casting specimen is to determine the discontinuities which influence the strength of Al wheel in an undesired way, especially the volumetric ones. To identify the dimensions of these discontinuities, exactly determine the application of accept/reject criteria.

2.5.1. X-Ray Inspection (Real Time Radioscopic Inspection)

RTR inspection is especially applied for the casting materials, which are produced for automotive, and airplane industry, acceptable defect type and defect size is so a few. Real time radioscopic method has been developed for the last few years and it is widely used in Al wheel production lines.

In this method, a feeding line from the casting machines to the RTR system transports the wheels and then, they pass through the inspection unit. In the system, the robotic manipulator, controlled by an operator or an automatic system, assists the operator to inspect all territories of the wheels effectively and to see clearly the defects on the monitor. As a result, the operator of the RTR system agrees to choose the accept or reject criteria for the inspected wheel. The typical image of Al wheel, which is obtained by means of real time radioscopic inspection system, is shown in Figure 2.16.

Aygün [37] explained the principles of RTR method in detail. The principles are familiar with radiography method. But, in this method the image is transferred to the monitor directly instead of the radiographic film and the evaluation is made by the means of monitor. Figure 2.17. shows the radioscopic inspection system.

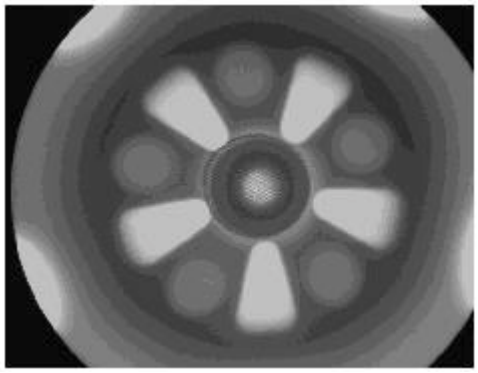

Figure 2.16. Real time radioscopic image of cast Al alloy wheel [44]

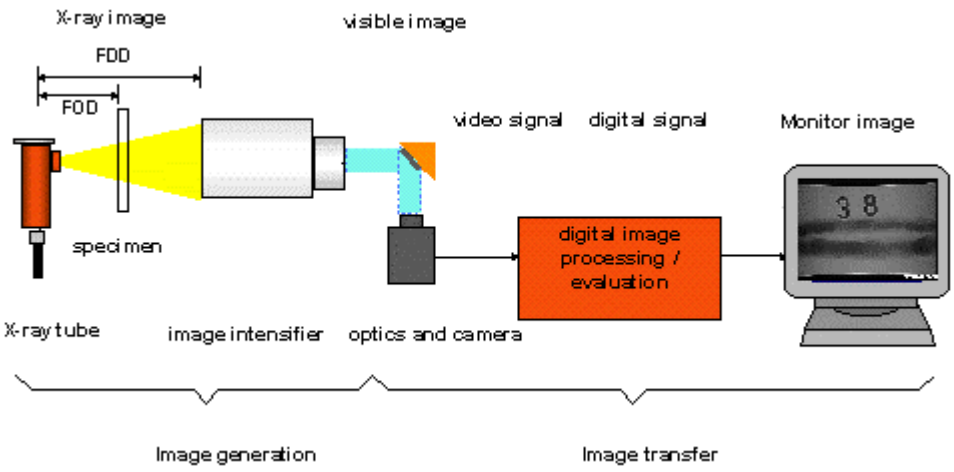

Figure 2.17. Radioscopic inspection system [45]

In the radioscopic system, the X-rays first pass through the specimen and reach to the image intensifier. The fluorescent screen takes place on the front surface of image intensifier and changes the X-rays to the electrons. Electrons are subjected to the exit as intensified by the lenses. The exit screen changes the electrons to the visible light by changing the wavelengths of them. A TV-camera, connected to the image intensifier, transfers the visible light to the monitor. The image on the monitor can be loaded into a video band or CD-Rom. The Object-to-Detector distance sets the geometric resolution or the resulting unsharpness in the radioscopic image. The relation between the Focus-to-Detector distance (FDD) and the Focus-to-Object distance (FOD) determines the

geometric magnification of the image. Figure 2.18. shows the schematic view of a RTR system that is used for inspecting the Al cast wheels.

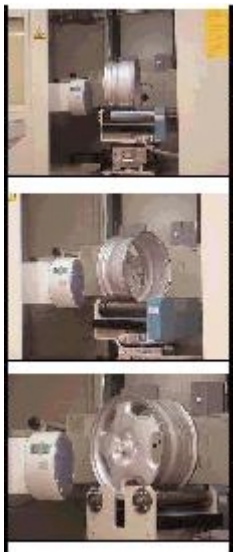

Figure 2.18. Schematic view of Al wheel inspecting RTR system [44]

The main parameters taken into account when producing the X-ray technique are, focal spot size of the X-ray tube head geometric distances between the tube head and the imaging device and the casting and the imaging device and X-ray energy level to be utilized, i.e. kV. and mA. The physical size of the focal spot (the area within the X-ray tube head that emits the X-ray beam) is a very important factor in determining resolution of the image. One factor that affects contrast of the X-ray image, is the photon flux density of the X-ray beam, which is mainly dependent on the mA level. The smaller the focal spot size the less photon flux produced. Therefore, a balance between focal spot size and the amount of mA utilized produces the optimum image quality. This is particularly important when inspecting light alloy castings. For light alloy castings the use of a tube head that has a variable focal spot can be an advantage. The tube head would need the capability of varying the focal spot from 70um to 300um [45,46].

In the early steps, investment cost is very high and this factor can be interpreted as it has a big disadvantage but on the other hand, for a long period, it is an economical and effective non-destructive testing method.

2.6. Quality Improvement of the Production

Quality improvement is the reduction of variability in processes and products. Reduced variability has directly translated into lower costs. Fewer repairs and warranty claims mean less rework and the reduction of waste of time, effort and money. Thus, quality is inversely proportional to variability. Excessive variability in process performance often results in waste.

If a product is to meet customer requirements, a stable or repeatable process should generally produce it. The process must be capable of operating with little variability around the target or nominal dimensions of the product quality characteristics. Statistical process control (SPC) is a powerful collection of problem solving tools useful in achieving process stability and improving capability through the reduction of variability [42,47,48]. SPC is the practice of using statistical methods to monitor and control a process. SPC allows users to take appropriate actions so that the process remains in a state of statistical control. It also gives users to improve the process ability to produce output that meets or exceeds customer expectations. After the monitoring of the process using SPC, various forms of feedback and feedforward regulation are used for process adjustment that is often called automatic process control (APC). Utilization of SPC with APC provides effective quality improvement.

To improve quality of the process, some tools can be used. These tools are called "**Quality Improvement Tools"** and given as [42,48,49,50]:

1. Process Flow Diagram
2. Cause and Effect (Fishbone) Diagram
3. Control Charts
4. Check Sheet
5. Pareto Diagram
6. Scatter Plot
7. Design of Experiments (DOE)
8. Histogram

Process Flow Diagram is a very useful tool to give brief information about the relationships between the process units (Fig.2.19.). Process flow diagram expresses detailed knowledge of the process and identifies the process flow and interaction between the process steps. Potential control points can also be identified.

Once a defect, error, or problem has been identified and isolated for further study, it is necessary to begin to analyze potential causes of this undesirable effect. In situations where causes are obvious or not, the **Fishbone Diagram** is a useful formal tool in unlayering potential causes (Fig.2.20.). By using this diagram, all contributing factors and their relationship are displayed and it identifies problem areas where data can be collected and analyzed.

Control Chart Analysis is a powerful tool to help monitoring quality in the process, to detect nonrandom variability, and to identify assignable causes [48]. A typical control chart is shown in Figure 2.21. It is a graphical display of a quality characteristic that has been measured or computed from a sample versus the sample number or time [51]. The chart contains a centerline that represents the average value of the quality characteristic corresponding to the in-control state. Two other horizontal lines, called upper control limit (UCL) and the lower control limit (LCL), are also shown on the chart. As long as the points plot within the control limits, the process is assumed to be in-control, and no action is necessary. However, a point that plots outside of the control limits is interpreted as evidence that the process is out of control and investigation and corrective action are required to find and eliminate the assignable cause or causes responsible for this behavior. There are some reasons for the popularity of control charts. Control charts provide reducing variability and monitoring performance over time. Also, by using control charts, trends and out of control conditions are immediately detected.

In the early stages of an SPC implementation, **Check Sheets** will often become necessary to collect either historical or current operating data about the process under investigation. A check sheet can be useful in this data collection activity. The check sheet shown in Figure 2.22. is for collecting the data of defects that occur on Al wheels. Check sheet simplifies data collection and analysis and spots problem areas by frequency of location, type or cause.

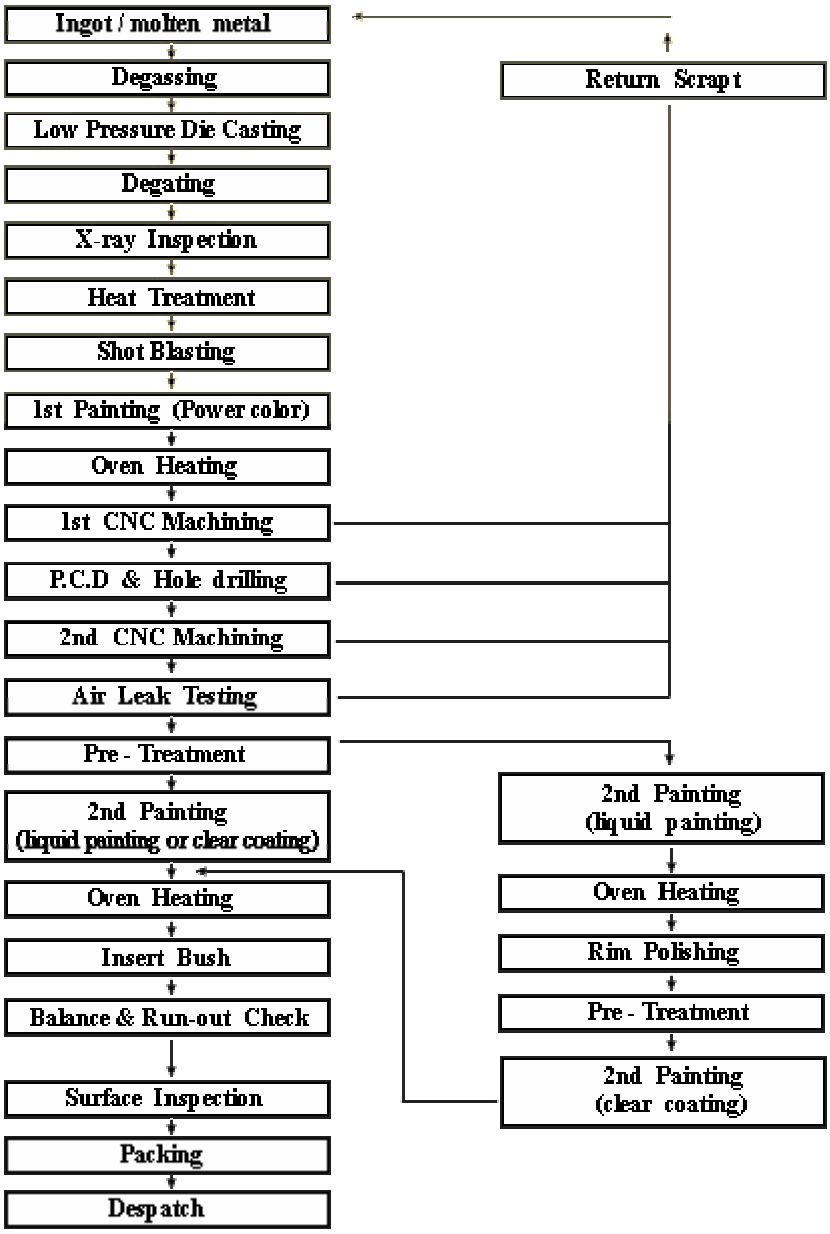

Figure 2.19. Process flow diagram of Al wheel production [11]

The Pareto Diagram is simply a frequency distribution of attribute data arranged by category. A Pareto diagram is shown in Figure 2.23. that includes the number of defects in a wheel production. It shows the total frequency of occurrence of each defect type against the various defect types. Hence, the causes of these defect types should probably be identified and attacked first. Also, various types of Pareto diagrams can be arranged with different types of data arrangement. Pareto diagram identifies the most significant problems to be worked and shows the vital few problems and factors. Moreover, it explains as the %80 of the problems is due to 20% of the factors.

Scatter Plot is a useful tool for identifying a potential relationship between two variables. Data are collected in pairs on the two variables, as (y,x), for i=1, 2,...,n. Then y values are plotted against the corresponding x. The shape of the scatter plot often indicates what type of relationship may exist between the two variables. The scatter plot, shown in Figure 2.24., indicates a positive correlation between temperature and pressure. By using this plot, a positive, negative or no relationship can be easily detected.

A Designed Experiment is a test or series of tests in which deliberate changes are made to the input variables of a process so that corresponding changes in the output response may be observed and identified. The process can be visualized as some combination of machines, methods and people that transform an input material into an output product (Fig.2.25.). This output product has one or more observable quality characteristics or responses. Some of the process variables X_1,X_2,...,Xp are controllable, and others, Z_1, Z_2, ..., Zp, are uncontrollable. Sometimes these uncontrollable factors are called “noise factors”. Design of experiment is useful in process development, trouble shooting, in engineering design and development. Also, magnitude and direction of important process variable effects can be identified and it greatly reduces the number of runs required to perform an experiment.

The Histogram represents a visual display of data (Fig.2.26.). Observed frequencies versus the number of defects are given in this histogram. The height of the each bar is equal to the frequency occurrence of the defects. The shape of histogram shows the nature of the distribution of the data. On this display, the central tendency (average) and variability are seen. And also, specification limits can be used to display the capability of the process [42,48,51].

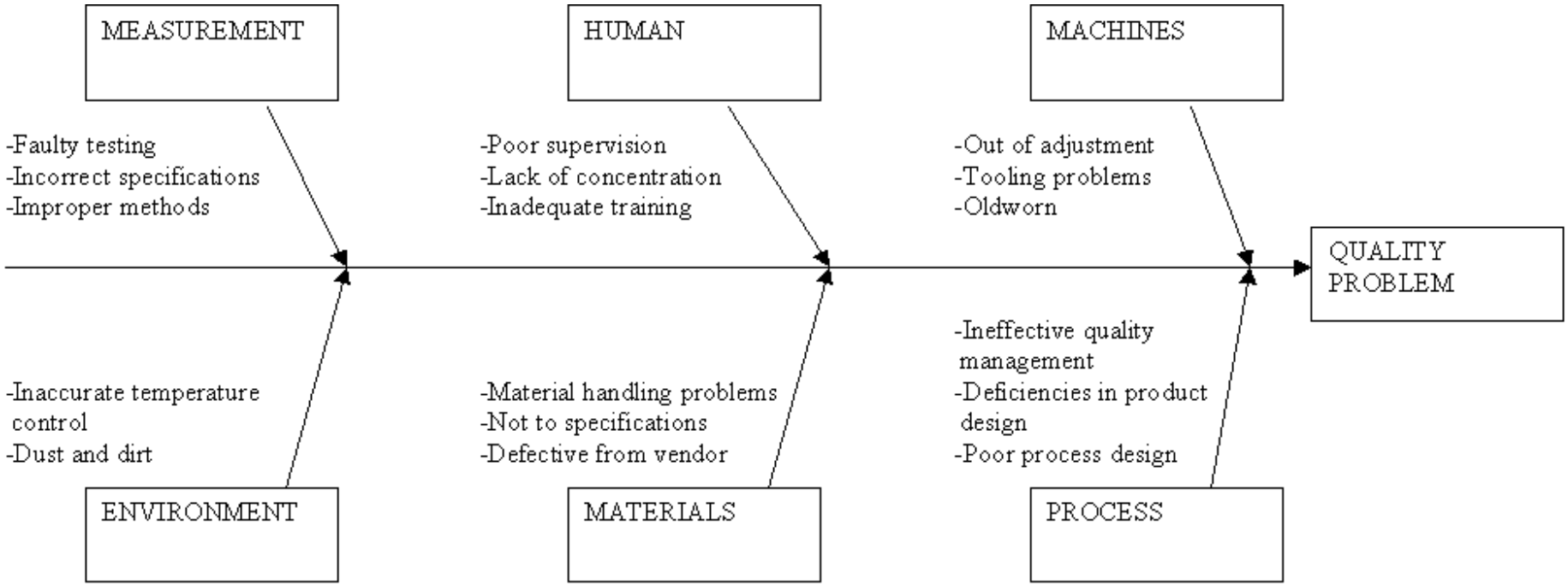

Figure 2.20. Fishbone diagram for quality problem

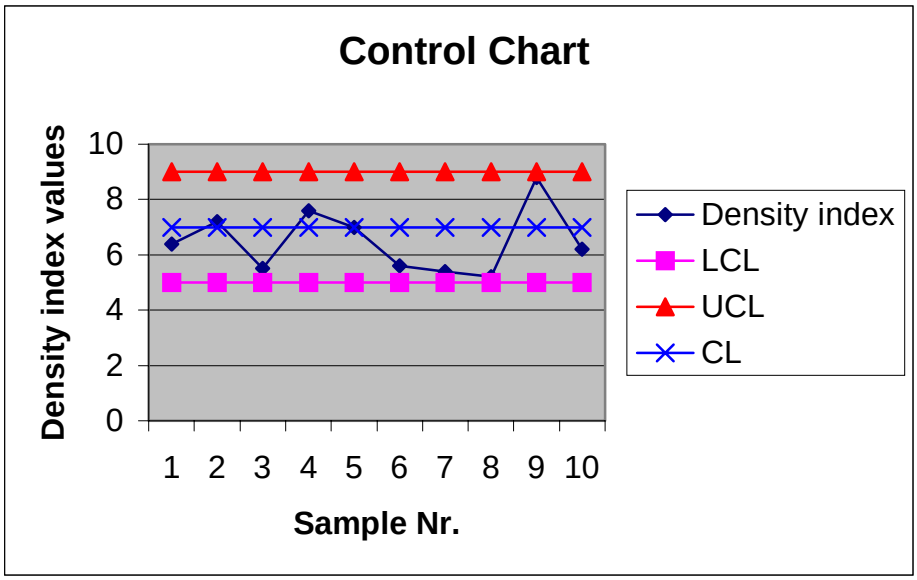

Figure 2.21. A typical control chart

	RTR			(C)	(minute)	Low Pressure Die Casting		
Number	Defect Types	Locations	Mold Number	Metal Temp.	Degass. Time	Cast. Time	Cast. Temp.	Cast.Press.

Figure 2.22. A check sheet to record defects on produced wheels

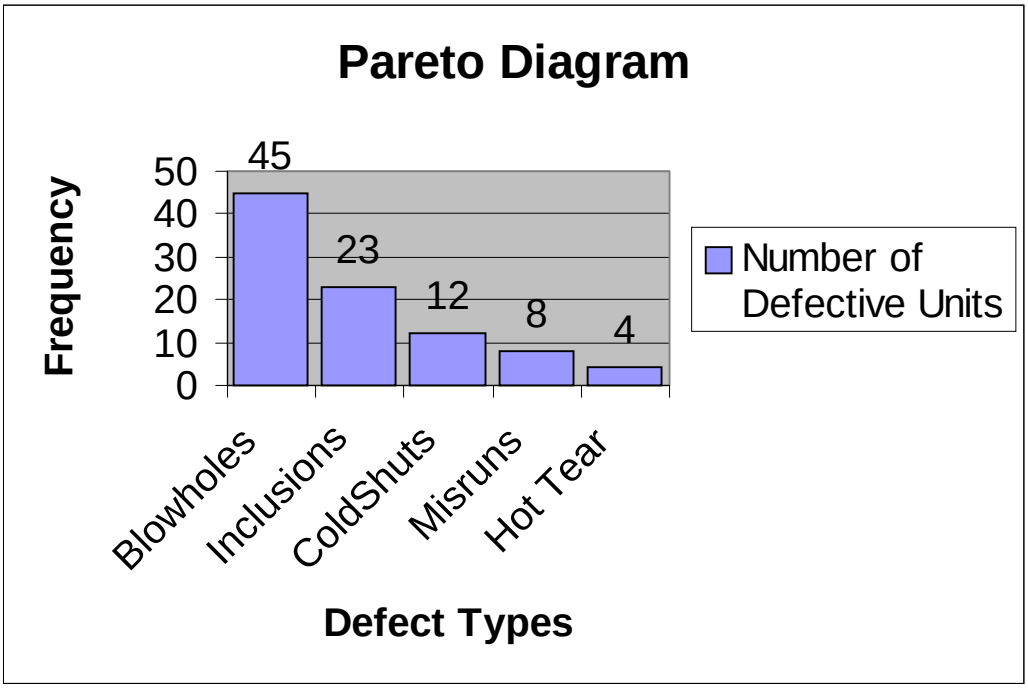

Figure 2.23. Pareto diagram of the defect data

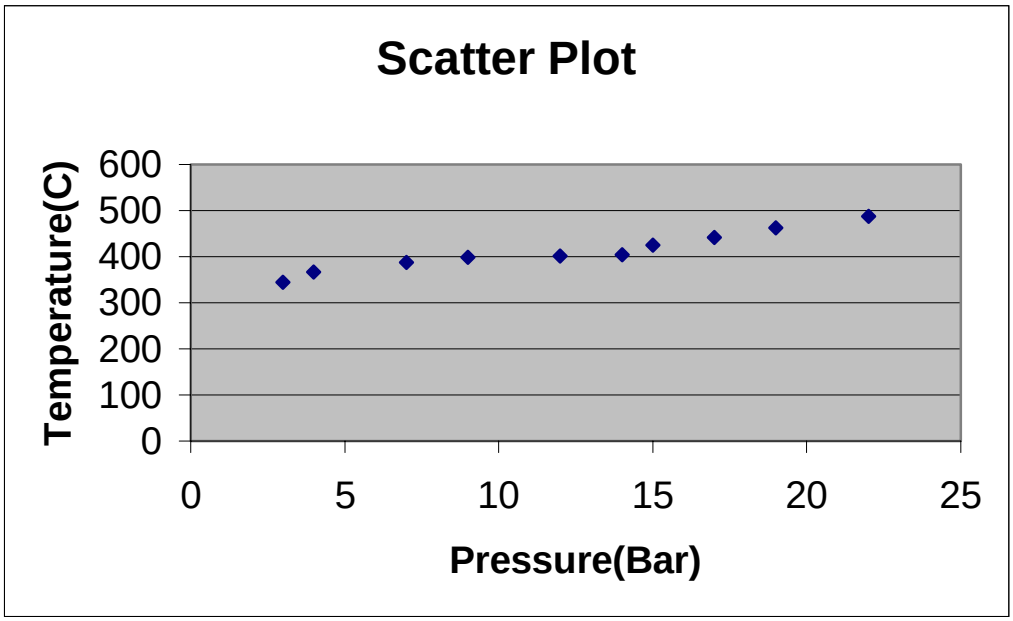

Figure 2.24. Scatter plot

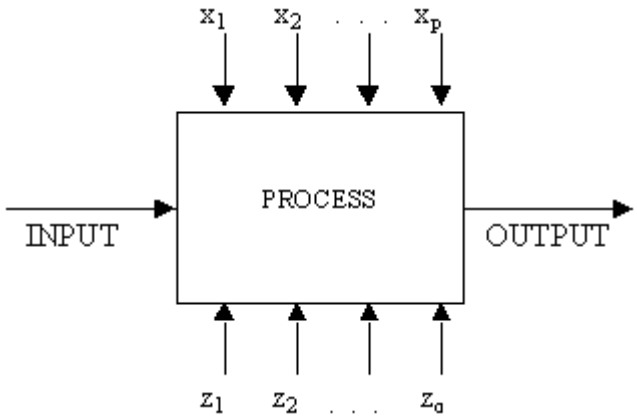

Figure 2.25. General model of a process [42]

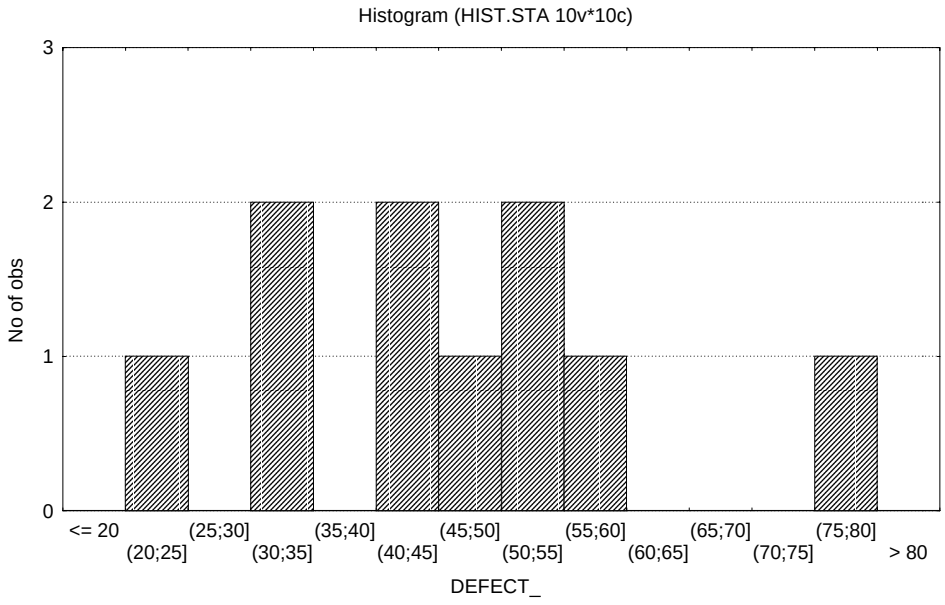

Figure 2.26. Histogram for measurements

CHAPTER 3

EXPERIMENTAL

This study has been realized by inspecting and evaluating the cast Al wheel production of a big casting plant. This plant has a entire cast aluminum wheel production line, including a shaft melting furnace, degassing unit, thermo analyzer, hydrogen content analyzer, low pressure die casting machines and real time inspection unit. Different types of aluminum wheels are produced on this line in different sizes and shapes.

3.1. Raw Material

Al-Si alloy ingots were used for the production of aluminum alloy wheels. These ingots were melt and die cast. As wheel casting alloy, DA 177 was used. The chemical composition of the alloy is given in Table 3.1.

Table 3.1. Chemical element compositions of DA 177

%Si	%Fe	%Cu	%Mn	%Mg	%Zn	%Ni	%Ti	%Sr	%Pb
10-11.7	max. 0.15	max. 0.02	max. 0.04	0.15-0.30	max. 0.04	max. 0.04	0.08-0.12	0.028-0.055	max. 0.03

Owing to the reasons explained in Chapter 2, for the production of aluminum casting alloy, this alloy type has been chosen. Also, scrapped wheels are melted with the normal ingots. DA 177 ingots are purchased from Aluwheel wil Bahrain Company and Dubai Aluminum Co. LTD.

3.2. Melting and Holding of Metal

A shaft type furnace (Striko Company production) was used to melt the Al-Si ingots. Melting and holding units are together in this type of furnaces. After the loading of ingots into the furnace, molten alloy is obtained in the melting bath part. The temperature of melting bath changes from 840°C to 890°C. Then, the molten metal is transferred to holding unit in the same furnace. The temperature of this part changes from 740°C to 790°C. According to the needs of die casting operators, holded molten

metal is transferred to the relevant die casting machine. But, before the transfer in the crucibles, degassing process are applied on the molten metal.

3.3. Degassing Process

Nitrogen gas is used during degassing process. Nitrogen gas is blown into the molten metal that is located in the crucible. Degassing pressure of nitrogen gas is about 0.4-0.6 bar. The temperature of degassing ranges between 715°C to 740°C. For realizing the homogeneous diffusion of nitrogen gas, it is transferred into molten metal with a 10-mm diameter shaft, as mixing the alloy by turning circumferentially. Duration of degassing is changeable and adjustable. But, in this study, period of degassing process was adjusted as 4 minutes. With degassing, there occurs a decrease in the amount of hydrogen gas that was entrapped in the molten metal. The application time of degassing changes with the properties of the molten metal. After degassing, some fluxes are put into the crucible to separate the slag and to achieve hydrogen equalizing. Then, samples taken from the crucibles are to be inspected by thermo-analyzer. Degassing unit had been purchased from Ford Green Engineering, LTD.

3.4. Analyzing of Molten Metal

By using thermo-analyzer equipment, some data that belongs to that sample can be collected. The equipment producer is Ideco Company and it analyzes the composition of alloying elements and the density of gas holes of the sample. Also, HYSCAN II, manufactured by Severn Science, analyzes the hydrogen gas change of the samples. In this study, the data of percentage of Ti and Sr, hydrogen gas change and density of gas holes could be collected according to the working conditions in the casting plant.

3.5. Low Pressure Die Casting

After sampling, molten metal is transferred to the crucible of the die casting machine. For each transferring, the transfer temperature value was collected. The crucible of the machine is under the die casting part, and by means of air pressure, the molten metal rises to the die and fills in. Then, low-pressure die casting process occurs. During die casting processes, the die casting temperature, pressure and injection time values were recorded. Die casting time is adjusted according to the size of the die. Also, for the first period of 7 seconds of the casting, the casting pressure is 160 mbar and it is

standard for all types of wheel dies. The dies are cooled by the help of air. Before casting, lubricants are applied by operators onto the die so that the aluminum wheel can easily leave the die, if it is necessary. Gima Company is the manufacturer of the low-pressure die casting machine and Striko Company manufactures the furnaces of die casting machines.

3.6. Real Time Radioscopic Inspection

After production, each aluminum casting alloy wheel is inspected by real time radioscopic inspection method at the end of the production line. Real time radioscopic inspections were performed with Philips MU31F. A 160 kV tube with a maximum tube current of 30mA has been used. As the x-ray image intensifier a CsI(Na) layered x-ray image intensifier tube has been used to convert photons to electrons, accelerate the electrons, and then reconvert them to light. And a CCD (Charge-coupled devices) camera has been used on real-time imaging system. The real-time radioscopy system contains two main components; the x-ray imaging system and the handling system. For handling the wheels an automatically programmable macro-manipulator with 6-axis has been used.

3.7. Construction of Graphics

The graphics were constructed by using computer software, as Excel and Statistica. Pie charts, Pareto diagrams, Scatter plots were obtained by using Excel. Normality plot and box whisker plots were constructed with Statistica.

CHAPTER 4

RESULTS AND DISCUSSIONS

In the present work, some relations between the process parameters and defect types and locations have been investigated by examining the process parameters and quality control results of aluminum wheel production. The results have been evaluated in three categories, process parameters, defects and effect of hydrogen content and density index on gas hole defects.

A flow chart has been constructed in order to reduce the number of scrap by providing feedback inside the production, and fishbone diagrams were used to understand the common influences on the production by achieving combination with the process model.

Using quality control results, defect types and their locations have been identified. The effects of hydrogen content and density index on gas hole defects have been determined. To describe the relationship between hydrogen content and density index, a model has been constructed. The validity of the graph has been checked by statistical approach. Finally, the influence of degassing time and the temperature of molten metal on the hydrogen content level of metal have been examined.

4.1. Process Parameters

As the process parameters, the temperature of the transferred metal to die casting machines, casting time, casting temperature, casting pressure have been evaluated. Also, according to the results of thermo-analyzer, compositions of Ti%, Sr%, density of the gas holes (DI) and hydrogen content have been considered. To observe the wheel production effectively, each type of moulds was noted. By using the combination of these values, types of defects and their locations have been determined at real time X-ray system.

Casting temperature, casting time and casting pressure have influences on the defect occurrence in aluminum cast wheels. Aygün [37] has stated that casting temperature has to be decreased in order to prevent microporosity. Also, G.J. Davies [22] have noted that the casting temperature must be reduced so that the shrinkage defects can be eliminated. To prevent both shrinkage and porosity defects, the optimum

casting temperature should be chosen during the process. The results of the production showed that the shrinkage defects were prevented by increasing casting temperature that provides more liquid metal to the shrink place during solidification. Due to the geometry of the die, in order to feed the metal through the spokes, which have thin sections, the casting temperature can be increased. Increasing casting temperature provides more fluidity during casting.

Also, casting pressure is outstanding for confronting the gas pore formation. Conley et al. [39] explain that the gas pore formation can form only when the gas pressure is adequate to overcome the total local external pressure. Therefore, the casting pressure should be adjusted for the casting process as outstandingly changing with the volume of the molten metal in the die, so that it can overcome the gas pressure of the metal.

Moreover, casting time greatly effects the formation of shrinkage defects on Al wheel. The results show that adjusting the casting time could eliminate the shrinkage defects. Also, Lee et al. [40] and Anson [41] reported that the solidification time affects the gas pore growth. With decreased solidification time, there becomes less time for hydrogen to diffuse from solidifying dendrite to the liquid. As G.J. Davies [22] informed that the attention had to be given to ensure that all parts of the casting are supplied with liquid metal during the whole of the solidification process, areas of liquid can become isolated. Consequently, the casting time should be adjusted to be optimum so that it will not tolerate for the appearance of shrinkage and porosity defects.

4.1.1. Feedback Control for Reducing Scrap

To prevent undesired scrapped wheels, minimize the number of scrap and improve the quality of the production, it is necessary to control all process parameters of cast Al wheel production. By realizing feedback control during production, the number of scrap wheels can be minimized. This can be done by adjusting and interfering the desired process parameters, which are out of control.

The schematic block diagram of control process is given in Figure 4.1. Process parameters can be changed within limits and quality of the process can be improved, according to the result of quality control. The quality control of the inspected wheels are divided as accepted and rejected. Using the results of quality control, the process parameters of the casting process are also adjusted. But the process control should cover all the steps of the production from the beginning to the end. The determination of the

types of defects on the rejected wheel provides a better understandable and exact control mechanism during the process. The related most influential process parameters should be given on the flow chart of production. For this purpose, a proposed flow chart for cast Al wheel production is established and shown in Figure 4.2.

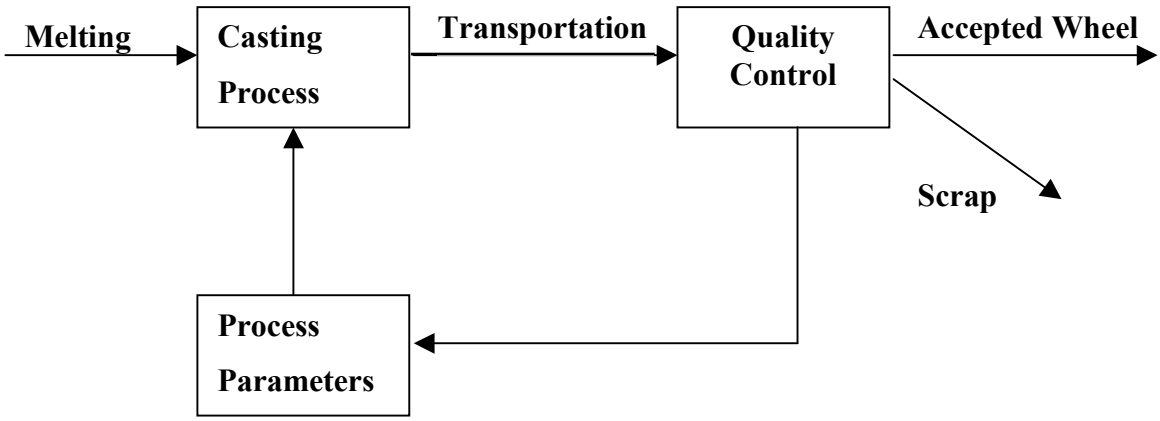

Figure 4.1. Block diagram of cast aluminum wheel production feedback

This new flow chart provides a more detailed and effective feedback control during the production. As a result of decision points and related process parameters, the adequate process adjustment can be realized on the exact process steps.

4.1.2. Proposed Flow Chart of Cast Al-Wheel Production

During the production, there are several control steps for achieving minimum scrap. Some of these steps include adjustments and feedbacks in order to reach a production without rejection.

For melting process, as shown in Figure 4.2., AlSi ingots and scrap Al-wheels are charged into the shaft type melting furnace and melted at above the melting temperature. After melting, to check the chemical composition, the chemical analysis is done. If the results are not as desired, charging alloy should be controlled. If the measured chemical composition is adequate, the molten metal is charged to crucibles. AlSr alloying material as waffle or rod and AlTiB master alloy as rod is added into each crucible to obtain desired composition. Sr helps the modification of AlSi alloys and Ti provides the grain refinement of the alloy. After the application of additives, it is necessary again to realize a chemical analysis so that the chemical composition can be

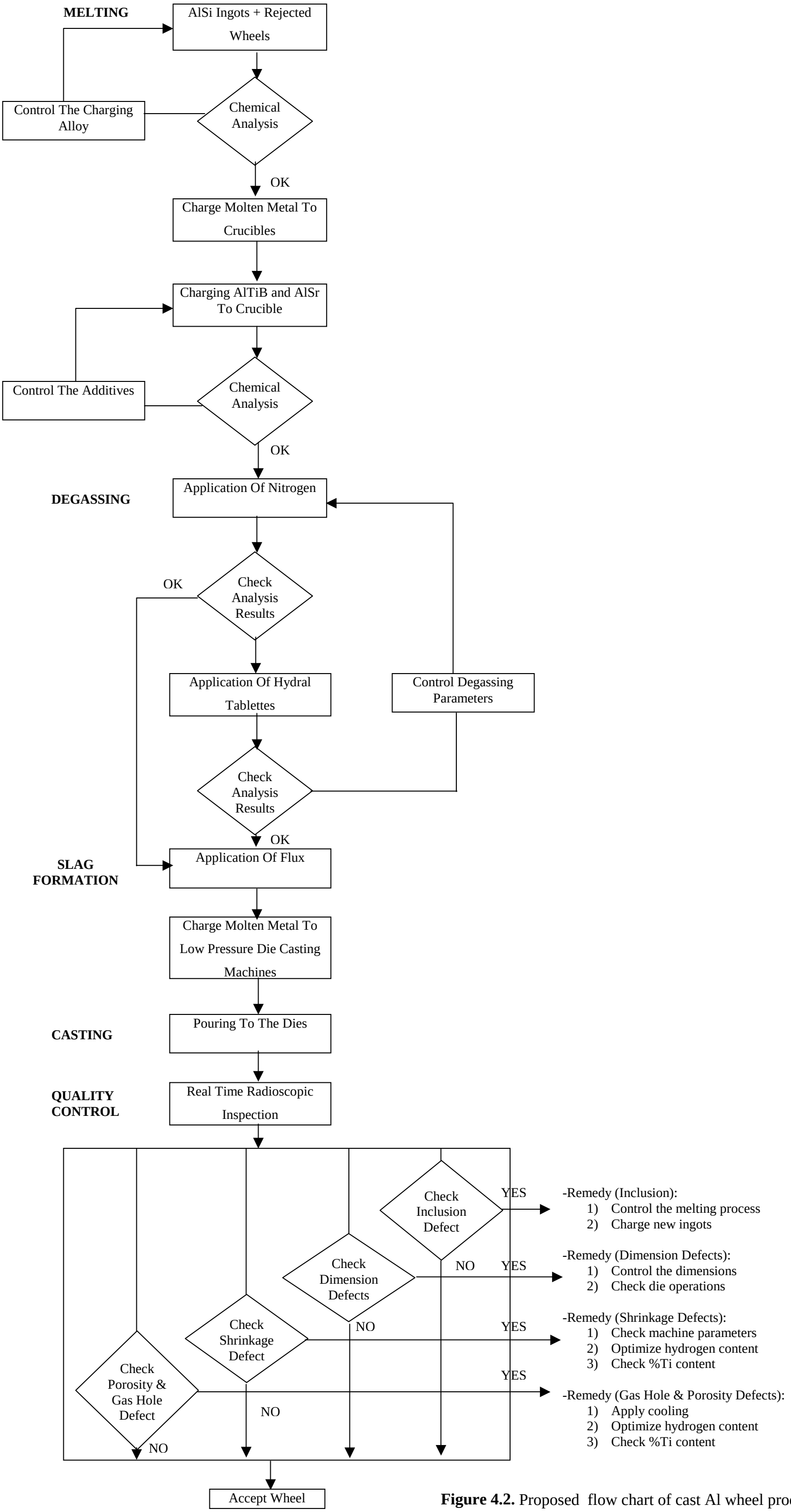

Figure 4.2. Proposed flow chart of cast Al wheel production

determined. If the chemical composition results are not suitable to the desired composition, the additives should be controlled.

Then the process passes to the step of degassing. To decrease the hydrogen content in liquid metal, nitrogen is applied to molten metal for a suitable period of time. After degassing, hydrogen content and density index values of the metal in the crucibles are measured. If the results are adequate, process passes through the step of slag formation. Otherwise, these values are regulated by the application of Hydral tablets (The tablets which are added to molten metal for increasing the hydrogen content) and an analysis for measuring hydrogen content and density index values are realized. To obtain desired hydrogen content, the degassing parameters should be controlled. Then, slag formation fluxes are added to the molten metal so that the slag can be got out to the surface of liquid metal and the slag on the surface are separated from the molten metal. Afterwards, the molten metal in the crucible is poured into the shot chamber of the low-pressure die casting machine. As following this step, after the metal is poured into the die, the casting process is completed by adjusting different casting pressure, time and temperature according to the size and shape of the wheel that will be cast.

All produced cast Al wheels are inspected by semi-automated real time radioscopic inspection system in the step of quality control. The wheels that have no or acceptable defects, pass through the following production steps such as mechanical cleaning, painting etc.. The rejected ones can be mainly defected as having porosity, gas holes, shrinkage, dimensional defects and inclusions.

To eliminate porosity defects and gas hole defects, the same remedies can be applied. If the porosity defects are encountered, cooling is applied during casting to the zone of defect occurrence. By this way, the porosity can be taken into the inside zones so that the porosity defect on the wheel can harm at least level. Also, Samuel et. al.[52] informs that formation of porosity is reduced with an increase in cooling rate. As latter, Lee et. al.[40] and Anson [41] reported that the solidification time effects the gas pore growth.

The main reason of porosity and gas hole defects is the trapped hydrogen gas in the molten metal. Samuel et. al. [52] reported that a higher hydrogen content will increase the porosity in the casting and the pore size, the amount of porosity increase with the initial hydrogen content in the melt. E.L.Rooy [53] explained that the hydrogen content must be controlled below the threshold levels corresponding to solidification conditions for both porosity and shrinkage defects. It means that hydrogen content

should be optimum so that it both provides the feedability of the metal and not being at high levels. Therefore hydrogen content occurs at low levels, the feedability of the alloy decreases. But if it is at high levels, it causes porosity and gas hole defects. The dissolved hydrogen level in melts is the main factor of gas porosity during solidification and it has to be avoided because it significantly decreases the mechanical and surface finish properties [19,54]. According to them, the hydrogen content must be optimized between minimum and maximum values in order to obtain both effective feeding and low hydrogen values. Consequently, optimizing hydrogen content can be achieved by controlling degassing step and if it is necessary Hydral tablets are added to supply feedability. Also, to adjust degassing time provides reducing the hydrogen content to the desired levels.

Grain refinement of the alloy reduces the amount of porosity and the application of Ti provides an improvement in the amount and distribution of porosity and shrinkage in the alloy [52]. L.Rooy [53] indicated that improved grain refinement of AlSi alloys provides feedability to reduce shrinkage tendencies and explains the porosity is caused by shrinkage and hydrogen. Consequently, it means that AlTiB master alloy provides the porosity decrease in metal. Therefore, to prevent porosity, Ti% content should be checked for minimized porosity.

The other most common defect type in Al-casting is the shrinkage. To prevent shrinkage the machine parameters of low pressure die casting machines, such as casting temperature, geometry of die, riser and gating system and cooling of the die have to be checked. The main reason for shrinkage defects is the lack of adequate feeding during casting process. Although G.J.Davies [22] informed that shrinkage defects could be eliminated by decreasing the casting temperature. However, during production of Al-wheels the casting temperature is increased in order to increase the feedability of molten metal through the spokes to the hub part that solidifies last and shrinkage is not formed at these sections.

Geometry of the die, its riser and gating system should be checked in order to eliminate shrinkage defects by means of increasing feedability characteristic. E.L. Rooy [53] reported that open risers are more effective than closed risers and riser mass and its position largely influence thermal consideration in order to control shrinkage. Samuel et. al. [52] explained that the combined geometry of a casting and its riser size influence on the thermal variables of the alloy that govern the feeding behavior of the casting.

Cooling of the die is the other important factor for preventing the appearance of shrinkage defects. E.L.Rooy [53] explained that hydrogen and shrinkage porosity are reduced by using chills or applying effective lubrication to correct the condition as means to apply cooling.

Optimizing the hydrogen content in the molten metal as mentioned before is another remedy for eliminating shrinkage defects. Hydrogen content should be optimized so that it provides easy feeding during casting.

Dimension defects occur on Al wheels as a result of unsuitable die dimensions and irregular die operations. These dimension defects can also be observed by visual examination. Especially, controlling the die patterns can eliminate wrong offset dimensions, diameter of wheel and other size defects that are relevant to the dimensions of the die. Also, some misalignment defects occur in terms of irregular die operations. If the dies are not entirely closed, it may cause the appearance of overmaterialed wheels. On the wheel, some unnecessary metal particles like chaplets take place, which are eliminated by checking the opening and closing of the dies.

Although, inclusions are not encountered too often in Al-wheels it is eliminated by controlling the melting process. The reason of the inclusions is the foreign materials that mix to the molten alloy during melting operations. Also, inclusions on the wheels generally occur when the raw material in the melting furnace reduces, and then the occurrence of inclusion increases. New ingot charging to melting furnace is necessary to prevent this event.

4.1.3. Parameters of Quality Evaluation

It is important to determine the factors that influence on the quality of Al-wheel in order to understand and to interpretative the wheel production. Some process parameters have great effects on the quality of the wheels. By determining these parameters, i.e., the key points, considerable quality of the production can be achieved. By the help of cause and effect diagrams, like Fishbone diagram, the process parameters, which have influence on the wheel production, are clearly and effectively revealed.

Figure 4.3. shows the Fishbone diagram, which includes some important process parameters, related to the production steps. According to each production step, as subclustered, the important process parameters are given. Meanwhile these parameters can be given in an other way, such as the main factors during production in Figure 4.4.

For example, casting conditions and molten alloy is important for low-pressure die-casting.

Process parameters are classified under four different main factors; measurement, human, materials and machines. Analyze results of hydrogen gas and composition of the molten alloy is important and has influence on the casting defects as measurement factor. Human factor greatly affects quality control process and adjustment of the machines. All the necessary materials used for the production are classified under the factor of materials as degassing gas, fluxes and the raw material. Also, the main systems that take place during the production of Al-wheel, are placed under the factor of machines.

During the die casting process, in every step of the process a check sheet is used as relevant to the production of each wheel. The pressure, temperature and the casting time have to be written down. After the inspection of each wheel these data should be interpreted in order to regulate the die casting of new wheels. Otherwise, determining the reasons of the defects can not be effectively realized as implemented currently.

For the pursuing of the manufactured wheels effectively, every wheel has to be coded with a special number by the operators of the casting machines. By using such a kind of code system, X-ray inspection operators can obviously inform the casting operators about the machine parameters.

In the quality control phase, inspection of the wheels should be done with an adequate speed to provide effective defect detection. Speed of the real time radioscopic inspection must be consistent, because if the inspection speed of the operator becomes slower, there occurs the clustering of the wheels on the inspection line. Then, to inspect all these overnumbered wheels, the operator increases inspection speed. On the other hand, if this speed is increased, insufficient and careless occurs. Also, careful attention should be given to the human environment where image interpretation takes place, to make it as conductive to correct, consistent image interpretation as possible. Measures should also be implemented to ensure that fatigue does not interfere with correct and consistent radioscopic image interpretation.

.

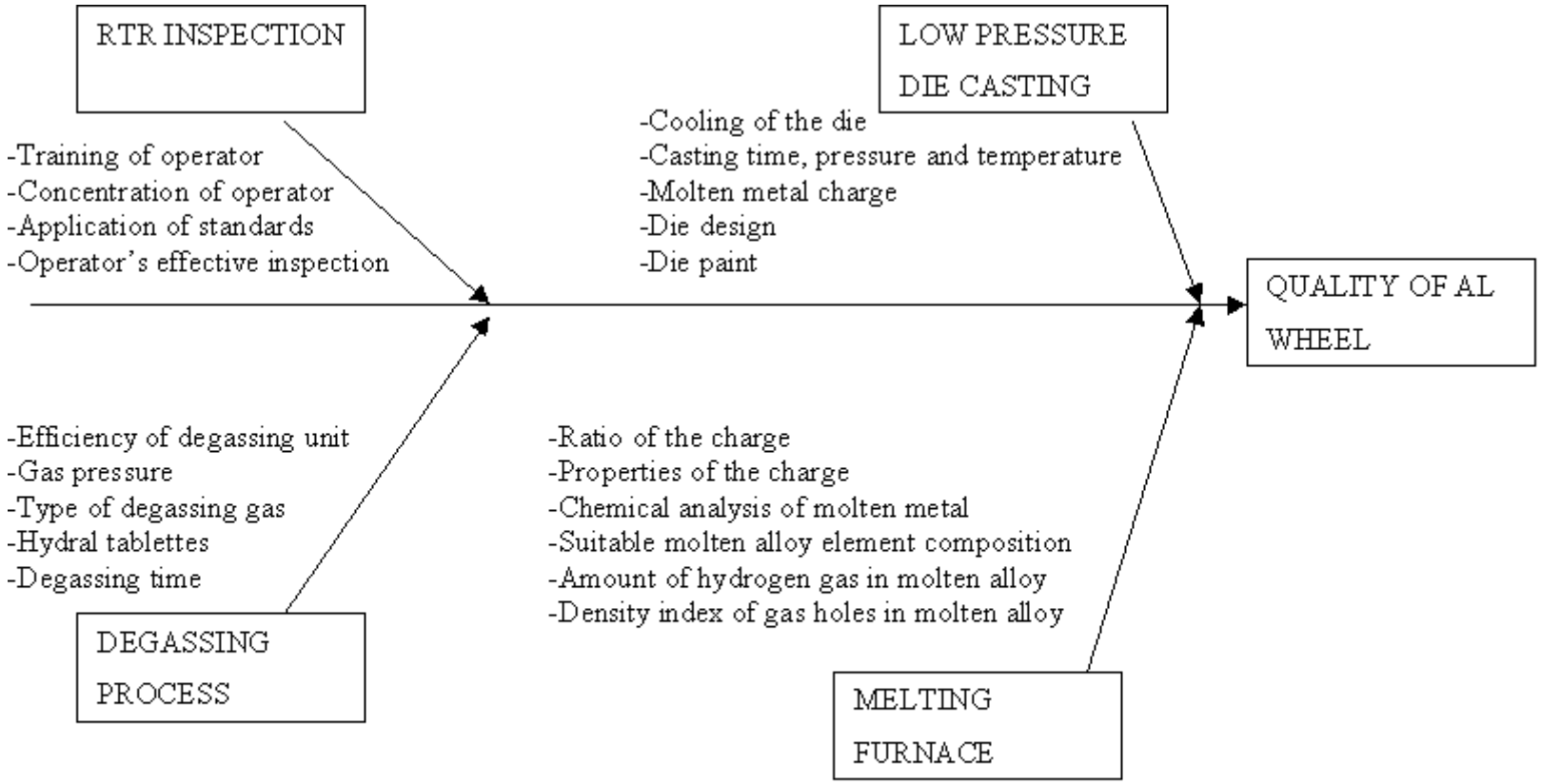

Figure 4.3. Fishbone diagram for the production steps that are affecting quality of cast Al wheel

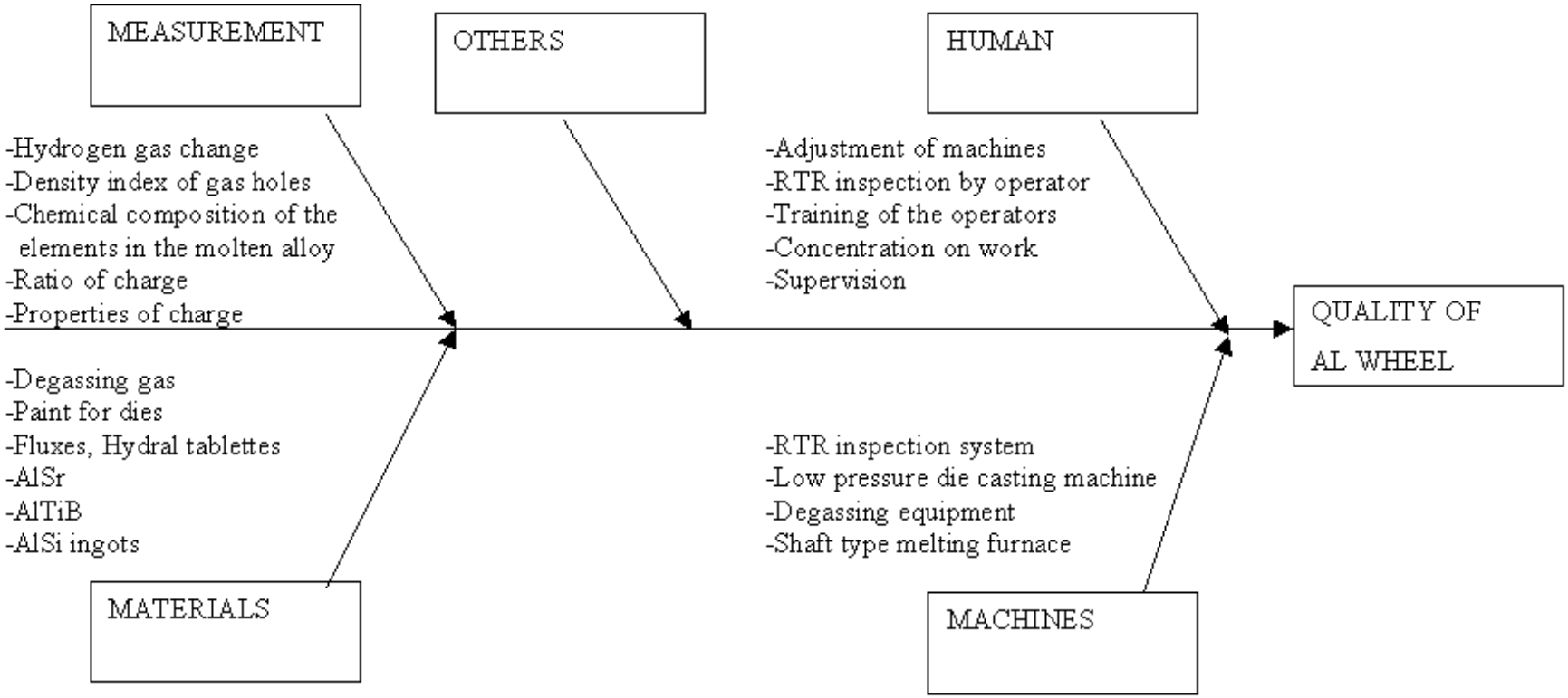

Figure 4.4. Fishbone diagram for the factors that are affecting quality of cast Al alloy wheel

4.2. Defect Types and Locations

In this study, total 5200 inspected by real-time radioscopy Al-wheels evaluated. Approximately 490 wheels have been rejected due defects that are not acceptable, which makes 9.4 scrap percentage of the production.

As the defects, gas holes, porosity and shrinkage have been focused and evaluated.

Types of Casting Defects:

To consistently produce high quality cast Al-wheels, the Al-Si alloy quality must be optimized prior to casting. One of the biggest problems in aluminum castings is porosity. Shrinkage type defects affect also mechanical and corrosion properties.

Figure 4.5. shows the types of casting defects that take place on the wheel. The wheels which have gas hole defects, porosity and shrinkage defects are 53%, 24% and 23% of the total number of 490 defected wheels, respectively. To apply the data on the chart, releases the types of defects that are encountered in the Al wheels. It is used to determine which defects are clearly considered as a cause of scrap wheels.

The main problem with quality of cast Al wheel occurs as gas holes and porosity as a result of trapped hydrogen gas in the molten metal as can be seen in the Figure 4.5.

Gas Holes:

When the hydrogen content of the melt exceeds the solubility limit, excess hydrogen forms gas bubbles. Figure 4.6. shows the pie chart relevant to the distribution of the locations of gas hole defects. According to the figure, gas hole defects are found as 74% on the spokes of the all gas hole defected wheels. Also, gas hole defects are occurred as 15% on the surface of the tire, as 7% on the hub and as 4% on the mounting parts of 249 wheels. By using this chart, the percentage of gas hole defected wheels can cleary be determined. Also, the chart assists to focus on which part of the wheel is sensitive for the gas hole defects.

Gas hole defects have been generally found on the spokes of the wheels. As the area of the spokes or the complexity of them increase, the probability of gas holes occurrence increases. Also, surface of tire has the large area for the mounting of tire and as the size of the wheel, also the area that surface of tire increases, gas hole defects can occur widely and with higher probability. First solidified metal on the mold wall prevents the gas removal.

Shrinkage:

Shrinkage occurs during solidification as a result of volumetric differences between liquid and solid state. For most aluminum alloys, volumetric shrinkage during solidification is about 6%. The locations of generally encountered shrinkage defects in 490 rejected wheels are shown in Figure 4.7. The pie chart shows that shrinkage defects are occurred as 97% on the hub part and as 3% on the surface of the tire of 115 wheels.

Shrinkage defects generally occur in the zone of hub. The main reason is the lack of feeding during solidification. A proper riser prevent shrinkage formation by maintaining a path for fluid flow from the higher heat mass and pressure of the riser to the encased liquid pool. Therefore the feeding of the die is achieved by the effective riser system, as located under the die and passing through the hub of the wheel. Hub part is the last solidified part of the wheel. By using chill or adjusting the die cooling system can also prevent shrinkage formation.

Porosity:

One of the biggest problems in aluminum castings is porosity, caused mainly by 1) shrinkage, resulting from the volume decrease accompanying solidification and 2) the evaluation of dissolved gases, resulting from the decrease in solubility of these gases in the solid as compared to the liquid metal. The hydrogen solubility limit in liquid aluminum alloys is considerably higher than for other gases and is strongly reduced in solid alloys; this means that gas porosity in aluminum alloys is mainly hydrogen porosity.

Porosity mostly occurs on the surface of the tire. The solidification rate and temperature gradient, which have on the kinetic nucleation and growth of the bubbles, influence the hydrogen porosity formation at the tire section. Rarely do the surface of tire region of small sized wheels have gas porosity. Especially, large sized wheels often have gas porosity due to larger surface area.

Evaluation of the defects has been done by Pareto diagrams. The number of defected wheels can be given as Pareto Diagrams as shown in Figure 4.8., Figure 4.9. and Figure 4.10. By the help of Pareto diagrams, the number of defected wheels are given as the number of quantity. According to these diagrams, it is understood that on which factors and matters have to been focused on. On the other hand, Pie charts give the rate of defected wheels according to the total number of defected wheels. Generally, Pareto diagrams show the total number of defected wheels and owing to this it is

determined that production is effective or not while Pie charts only show the type of defected wheels as a percentage of the all produced wheels.

Figure 4.8. shows the distribution of defect types as the number of defected cast Al wheels. During this study, 249 gas hole defected wheels, 114 porosity defected wheels and 115 shrinkage defected wheels of total 490 inspected wheels have been encountered. The remain defected wheels have misalignment which is dimensional defect. This figure was constructed in order to determine the number of defected wheels according to the defect types that they have and it helps to understand the most critical zones for defect occurrence.

In Figure 4.9., the Pareto diagram shows the locations of gas hole defect as the number of gas hole defected wheels. As it can be seen from the figure, gas hole defects generally take place on the spokes as the quantity of 184. Also, there are 39 wheels with gas hole defects on the surface of tire, 19 defected wheels on the hub and finally 7 wheels defected on mounting parts of the wheel. This diagram shows the classification of quantity of the wheel which have gas hole defects according to the occurrence locations on the wheel. By this way, it gives the most important regions for gas hole defect appearance. The diagram informs that for gas hole defects, it is necessary to consider and to take care about the design of the spokes and the size, complexity of the wheel.

The number of shrinkage defected wheels according to the locations on the wheel is given in Figure 4.10. It shows that there are 107 wheels that have shrinkage defects on the hub region of the wheel and a few, 4 wheels with shrinkage defect on the surface of tire. This diagram obviously gives the number of defected wheels according to the defect locations and assists to focus on the important regions that have to be considered for preventing shrinkage defects. Here, it is understandable to focus on the hub region of the wheels as critical for shrinkage defects.

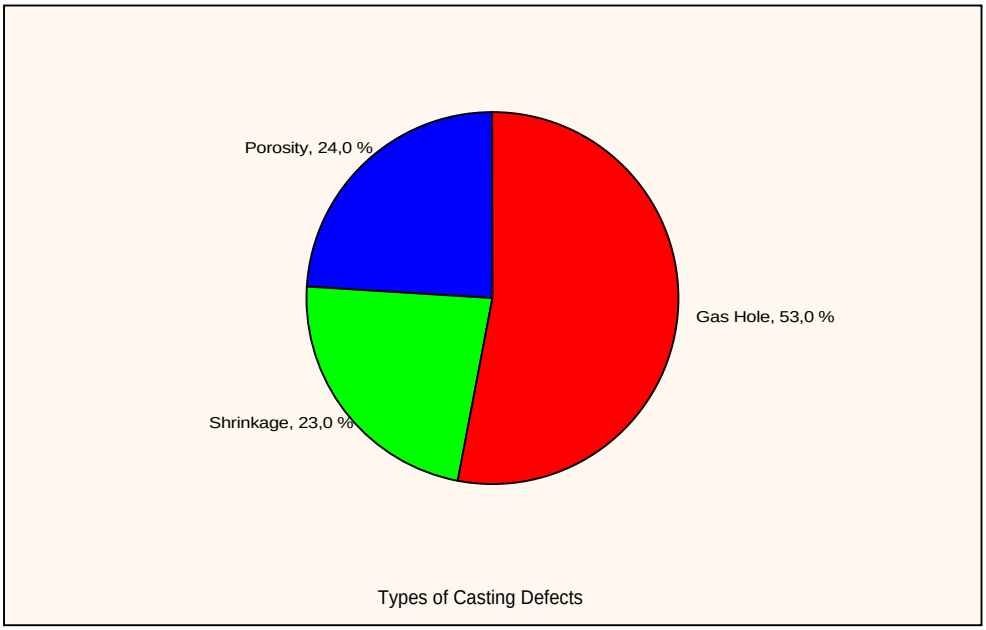

Figure 4.5. Types of casting defects encountered on cast Al wheels

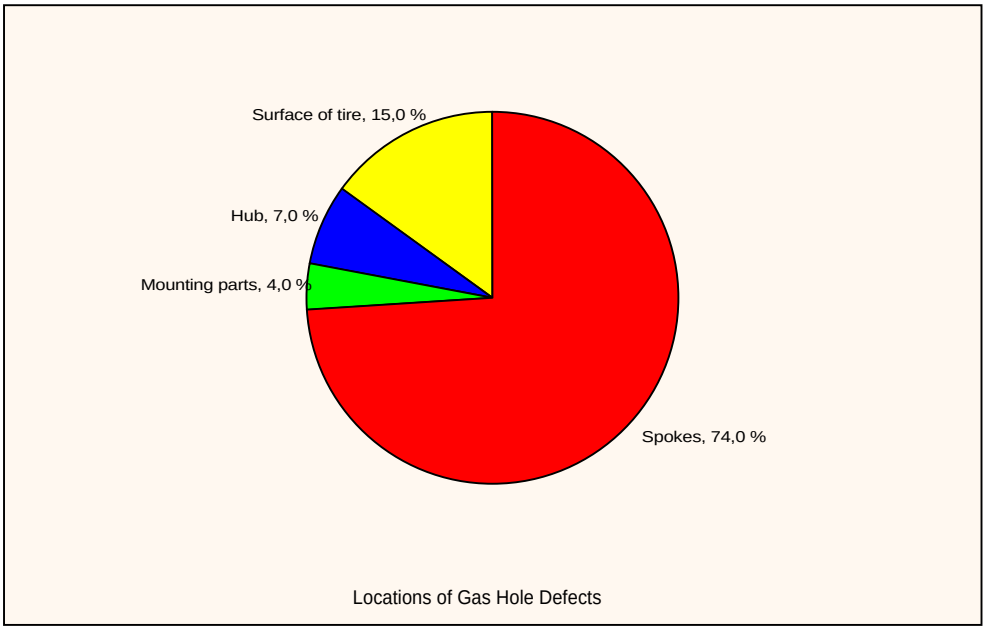

Figure 4.6. Locations of gas hole defects encountered on cast Al wheels

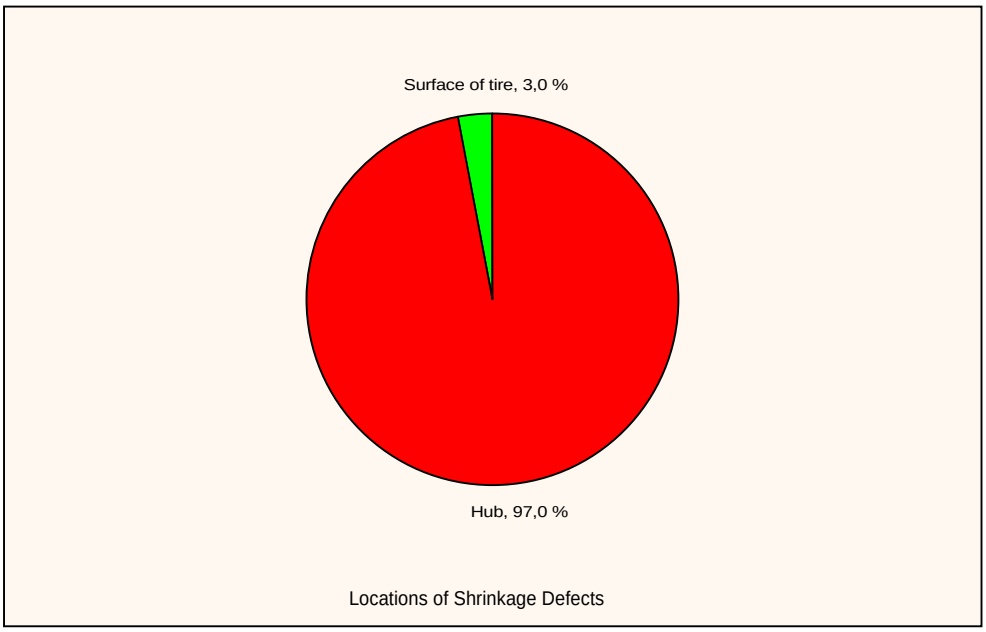

Figure 4.7. Locations of shrinkage defects encountered on cast Al wheels

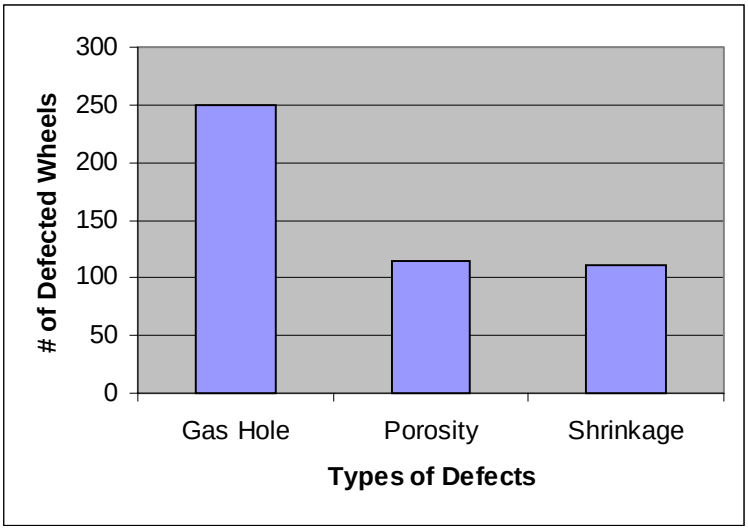

Figure 4.8. Pareto diagram of defect types that appear on cast Al wheels

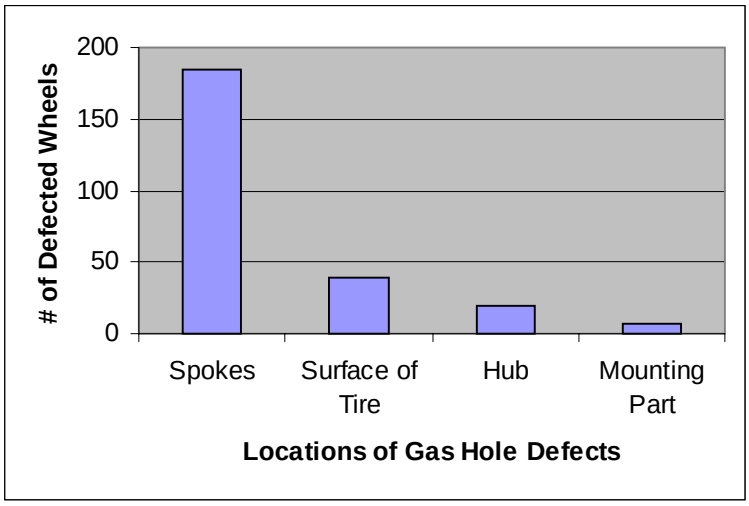

Figure 4.9. Pareto diagram of the gas hole defects' locations

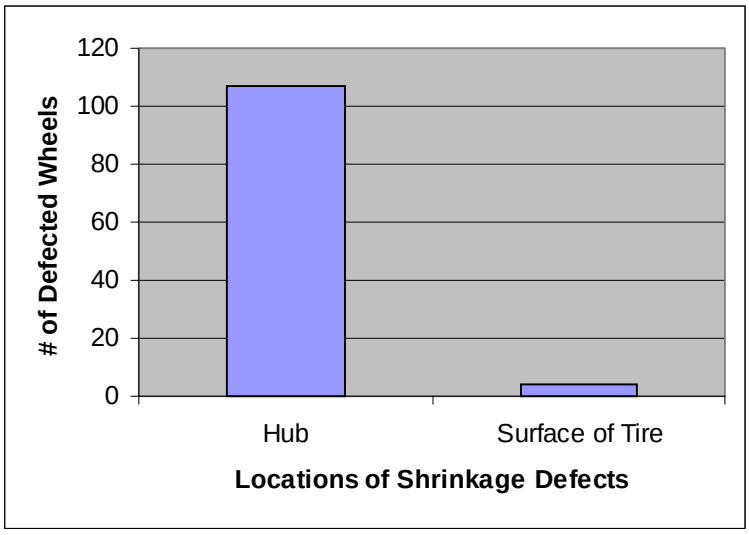

Figure 4.10. Pareto diagram according to the locations of shrinkage defects

4.3. Hydrogen Content and Density Index Factor on Gas Hole Defect

To determine the apparent correlation between gas hole and/or porosity and hydrogen content (The amount of hydrogen in aluminum alloy) for the inspected wheels, the hydrogen content in molten metal and density index (Differential density rate of Al which determines the porosity level of the molten metal) data were collected and then, the real time radioscopic inspection results have been evaluated for gas pores and porosity defects.

For density index of gas holes and hydrogen content value, three different graphics have been constructed and each graphic shows the data for one observation. With three observations, more exact results could be achieved. During 3 different time periods, for the same die casting machine, die and type of die, the hydrogen content and density index values were taken relevant to the gas hole defected wheels. Each observation contains the data related to each time period. Then, the data belonged to each observation were used to construct figures in order to show the number of defected wheels against density index and hydrogen content values as separately.

Figure 4.11. shows the change of number of defected wheels according to the hydrogen content in molten metal for the first observation. In this figure, it is clear that the gas hole defected wheels cluster between the hydrogen amount of 0.025cc/100gr and 0.27cc/100gr.

Figure 4.12. belongs to the number of defected wheels according to the hydrogen for the second observation. From the figure, it is determined that the defected wheels occur between the hydrogen content level of 0.02cc/100gr and 0.05cc/100gr, and at the level of 0.04cc/100gr.

For the third observation, (Fig. 4.13.) the change of amount of defected wheels as versus to the hydrogen amount in molten metal. It is seen that the gas hole defected wheels appear between the hydrogen amount of 0.04cc/100gr and 0.27cc/100gr..

According to these three graphics, the hydrogen content interval between 0.02cc/100gr and 0.27cc/100gr has large number of defected wheels.

A more exact evaluation of hydrogen content in molten metal can be made by density index measurements of uncut samples. The higher the density index of the sample, the higher the porosity levels. Figure 4.14., Figure 4.15. and Figure 4.16., combinely show the number of defected wheels against the density index of gas holes and/or porosity in the molten metal. Figure 4.14. shows the clustering of gas hole defected wheels according to the density index of gas holes for the first observation. For

this observation, the defected wheels have %density index values between the intervals of 1.5 to 4.5 and 6.3 to 12.2.

For the second observation, (Fig. 4.15.), defects mostly occurred at the DI% values from 1.2 to 3.6.

Finally, in the third observation, (Fig. 4.16.) the defected wheels take place between the DI% intervals of 1 to 2.5 and 4.5 to 10.

By the interpretation of these graphics, it may be said that the DI% values of intervals from 1.5 to 3 and 6 to 12, can have the large number of gas holes and/or porosity defected wheels. Although, the collected data for the evaluation is adequate, the more data that can be collected may give an exact result related to the effect of density index interval on the number of defected wheels.

Also, the research about the hydrogen content in the molten metal and the charging order of the crucible showed that for the same die casting machine system, with the higher hydrogen content, anomaly less number of defected wheels are observed as shown in Figure 4.11., Figure 4.12. and Figure 4.13.

In Figure 4.11, between the hydrogen amount of 0.18cc/100gr and 0.25cc/100gr, there seems to be more number of defected wheels appears than the higher hydrogen amounts. Also, again from the Figure 4.12., it can be understood that below the hydrogen amount of 0.05cc/100gr, more number of defected wheels has examined than the higher values. For the third observation, in 4.13., it shows that more number of defected wheels occur between hydrogen amount of 0.04cc/100gr and 0.27cc/100gr. And the number of defected wheels is much more in these lower values than the higher values of hydrogen content.

Normally, the number of defected wheels increases as the hydrogen in the molten metal increases. However, a permanent die may require metal with a fairly high gas content to produce acceptable castings. In such a case, both a minimum and maximum gas content should be specified.

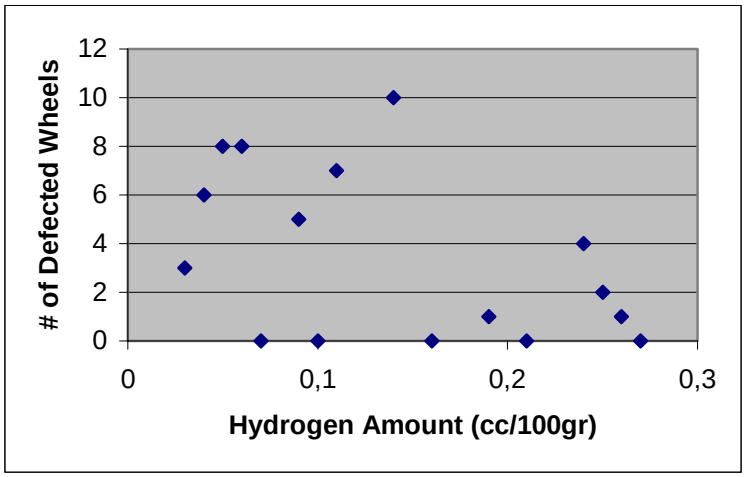

Figure 4.11. Number of defected wheel change according to hydrogen content at 1st observation

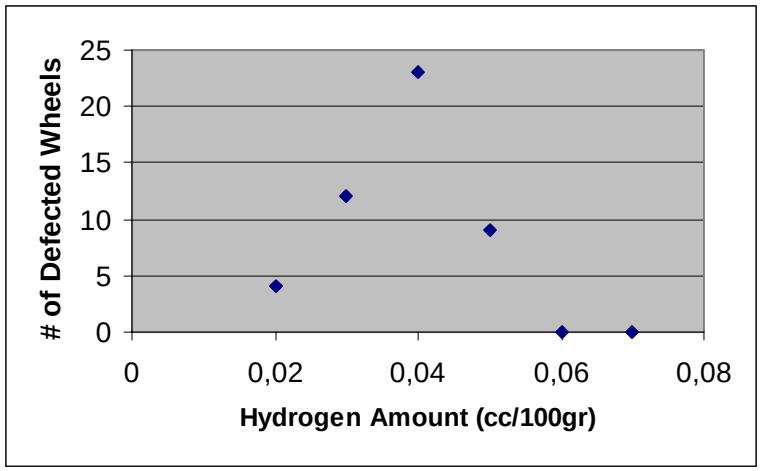

Figure 4.12. Number of defected wheel change according to hydrogen content at 2nd observation

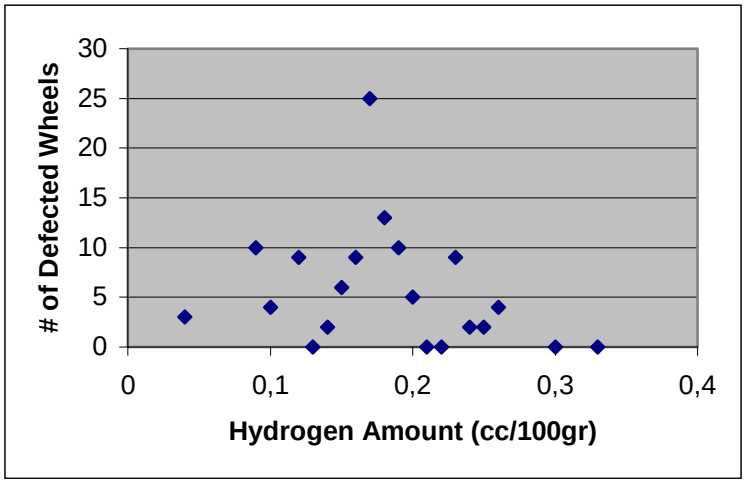

Figure 4.13. Number of defected wheel change according to hydrogen content at 3rd observation

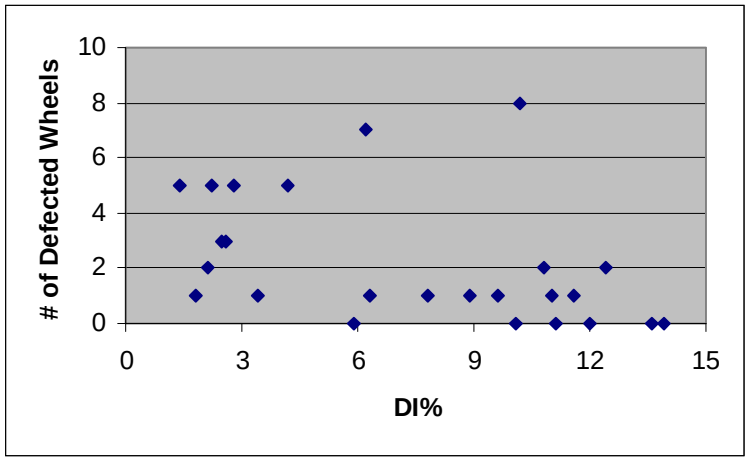

Figure 4.14. Number of defected wheel change according to density index factor at 1st observation

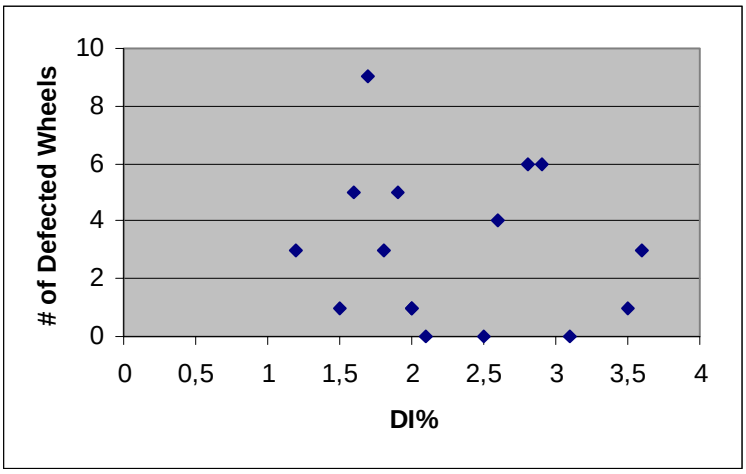

Figure 4.15. Number of defected wheel change according to density index factor at 2nd observation

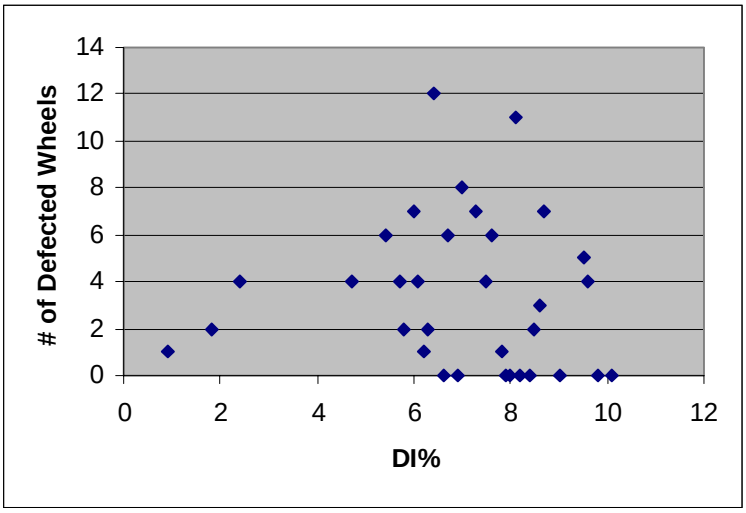

Figure 4.16. Number of defected wheel change according to density index factor at 3rd observation

4.3.1. Relation between Hydrogen Content and Density Index Factor

To find a relation between the density index and hydrogen content in molten metal a Scatter diagram was used. Figure 4.17. shows the relation between these two variables, constructed by using data given in Table A.1. in Appendix. Also, it is possible to apply a model for these variables in order to predict the relation between them.

As it can be observed from the figure, the density index values and hydrogen amount of molten metal are highly autocorrelated and there is a linear positive relation between these two variables. Owing to this, the fitted value of this model for hydrogen content and DI% can be found by using Least Square Method [42,55]. During this study, for the calculation of matrices, computer software Excel and Statistica were used.

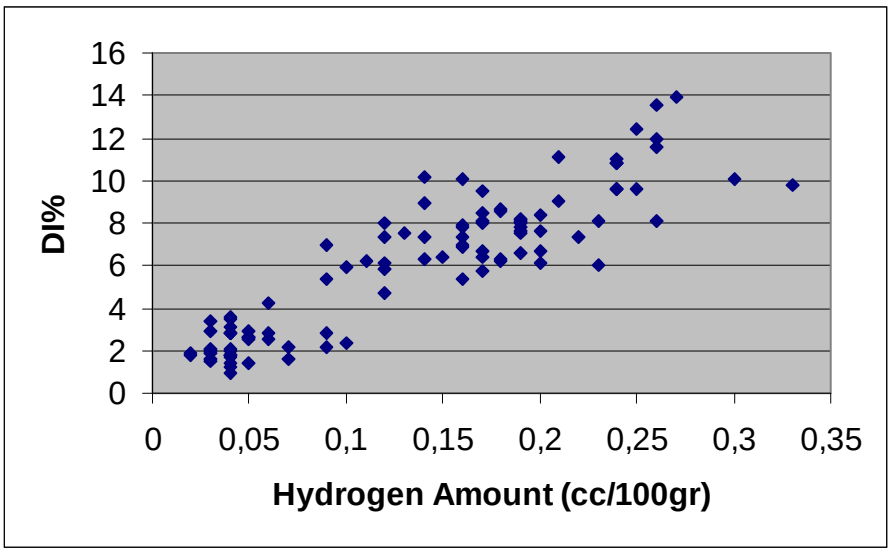

Figure 4.17. The relation between hydrogen content and density index factor

4.3.2. Relationship between Hydrogen Content and Density Index by Using Least Square Method

To find the linearity of hydrogen content and density relationship least square method was applied.

The parameters in autoregressive models can be estimated by the method of Least Squares. It is supposed that the model is [42,55],

$$y = \beta_0 + \beta_1 z + \varepsilon \qquad (4.1)$$

where z is the hydrogen content values in molten metal, y is the density index values of gas holes, β_0 and β_1 are the coefficients and ε is the residual value. By choosing the values β_0 and β_1, it minimizes the sum of squared errors.

The values of density index and hydrogen content values are given in Table A.1. in Appendix. Then the two data matrices for density index values **Y** and hydrogen contents **Z** are shown as,

$$\mathbf{Y} = \begin{bmatrix} DI_{11} \\ DI_{21} \\ DI_{31} \\ . \\ . \\ . \\ . \\ DI_{1001} \end{bmatrix}_{100x1} \qquad \mathbf{Z} = \begin{bmatrix} 1 & H_1 \\ 1 & H_2 \\ . & . \\ . & . \\ . & . \\ . & . \\ 1 & H_{100} \end{bmatrix}_{100x2} \tag{4.2}$$

Notice that the first column in the **Z** matrix is a column of 1's. Also, a particular data point is identified by specific rows of the **Y** and **Z** matrices. Using this notation, the general linear model can be expressed in matrix form as,

$$\mathbf{Y} = \mathbf{Z} \times \boldsymbol{\beta} + \boldsymbol{\varepsilon} \tag{4.3}$$

The $\hat{\boldsymbol{\beta}}$ matrix shown in the box contains the least squares estimates which provides to obtain the coefficients β_0, β_1 of the linear model.

$$\hat{\boldsymbol{\beta}} = \begin{bmatrix} \beta_0 \\ \beta_1 \end{bmatrix} \tag{4.4}$$

The residual matrix is the matrix of the errors that are the differences between the original density index values and the estimated ones by using the model. The residual matrix is,

$$\boldsymbol{\varepsilon} = \begin{bmatrix} \varepsilon_1 \\ . \\ . \\ \varepsilon_{100} \end{bmatrix} \tag{4.5}$$

Using the **Y** and **Z** data matrices as given in Equation (4.2), their transposes and the $\hat{\boldsymbol{\beta}}$ matrix, least square equations can be written as,

$$\left(\mathbf{Z}' \times \mathbf{Z}\right) \times \hat{\boldsymbol{\beta}} = \mathbf{Z}' \times \mathbf{Y} \tag{4.6}$$

Thus, $(\mathbf{Z}'\times\mathbf{Z})$ is the coefficient matrix of least squares estimates $\hat{\beta}_0$ and $\hat{\beta}_1$. The solution is,

$$\hat{\boldsymbol{\beta}} = (\mathbf{Z}' \times \mathbf{Z})^{-1} \times \mathbf{Z}' \times \mathbf{Y} \tag{4.7}$$

Then, the model becomes as,

$$\mathbf{Y} = \beta_0 + \beta_1 \times \mathbf{Z} + \boldsymbol{\varepsilon} \tag{4.8}$$

And the solution to the least squares is due to Equation (4.7),

$$\hat{\boldsymbol{\beta}} = \left(\begin{bmatrix} 1 & 1 & . & . & 1 \\ H_1 & H_2 & . & . & H_{100} \end{bmatrix}_{2x100} \times \begin{bmatrix} 1 & H_1 \\ 1 & H_2 \\ . & . \\ . & . \\ 1 & H_{100} \end{bmatrix}_{100x2} \right)^{-1} \times \begin{bmatrix} 1 & 1 & . & 1 \\ H_1 & H_2 & . & H_{100} \end{bmatrix}_{2x100} \times \begin{bmatrix} DI_1 \\ DI_2 \\ . \\ DI_{100} \end{bmatrix}_{100x1}$$

$\hat{\mathbf{a}}$ is obtained by putting the data into the equation,

$$\hat{\boldsymbol{\beta}} = \begin{bmatrix} 100 & 13.43 \\ 13.43 & 2.4399 \end{bmatrix}_{2x2}^{-1} \times \begin{bmatrix} 600.2 \\ 104.243 \end{bmatrix}_{2x1}$$

Then,

$$\hat{\boldsymbol{\beta}} = \frac{1}{63.6251} \times \begin{bmatrix} 2.4399 & -13.43 \\ -13.43 & 100 \end{bmatrix}_{2x2} \times \begin{bmatrix} 600.2 \\ 104.243 \end{bmatrix}_{2x1}$$

$$\hat{\boldsymbol{\beta}} = \begin{bmatrix} 1.013 \\ 37.15 \end{bmatrix}_{2x1}$$

Therefore the values of coefficients are found as,

$\hat{\beta}_0 = 1.013$ and $\hat{\beta}_1 = 37.15$

Thus the predicted Equation (4.8) is,

$$\hat{y} = 1.013 + 37.15z$$

In order to understand whether this predicted equation is suitable or not, it is necessary to calculate the random errors. $\hat{\mathbf{Y}}$ matrix shows the calculated values of predicted density index of gas holes. The equation is,

$$\hat{\mathbf{Y}} = \mathbf{Z} \times \hat{\boldsymbol{\beta}} \tag{4.9}$$

where $\hat{\boldsymbol{\beta}}$ is the estimates of the coefficients as $\hat{\beta}_0$ and $\hat{\beta}_1$. Performing the multiplication,

$$\hat{\mathbf{Y}} = \begin{bmatrix} 1 & 0.07 \\ 1 & 0.09 \\ . & . \\ . & . \\ 1 & 0.12 \end{bmatrix}_{100x2} \times \begin{bmatrix} 1.013 \\ 37.15 \end{bmatrix}_{2x1} = \begin{bmatrix} 3.6135 \\ 4.3565 \\ . \\ . \\ 5.471 \end{bmatrix}_{100x1}$$

the predicted values for density index values are found. As given in the following equation, the residuals are calculated by subtracting the predicted density index matrix from the original density index values given as **Y** matrix;

$$\hat{\boldsymbol{\varepsilon}} = \mathbf{Y} - \hat{\mathbf{Y}} \tag{4.10}$$

Therefore, $\hat{\boldsymbol{\alpha}}$ is obtained,

$$\hat{\boldsymbol{\varepsilon}} = \begin{bmatrix} 2.2 \\ 2.8 \\ . \\ 4.7 \end{bmatrix}_{100x1} - \begin{bmatrix} 3.6135 \\ 4.3565 \\ . \\ 5.471 \end{bmatrix}_{100x1} = \begin{bmatrix} -1.41 \\ -1.55 \\ . \\ -0.771 \end{bmatrix}_{100x1}$$

Then, the predicted values of the residuals as given in $\hat{\boldsymbol{\varepsilon}}$ matrix, are adapted to the normality plot as shown in Figure 4.18. All the residual values and applied data are given in Table A.1. in Appendix. According to the figure, it can be said that the residuals distribute normally and there is a relation between hydrogen content and density index.

To determine the model applied to data is suitable or not, the mean value of these residuals and their autocorrelation values according to the lags should also be checked. As the mean of residuals has a value close to zero, it can be told that the predicted equation is true. The mean of the residuals was calculated as –0.00024 by applying the data that were obtained from the predicted equation. This mean value is so close to zero and it can be concluded that the model is useful for the data.

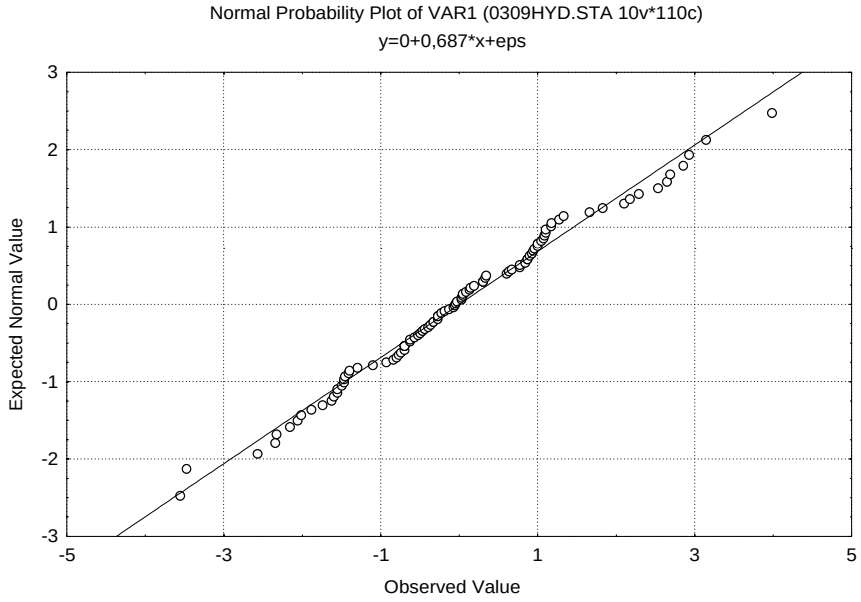

Figure 4.18. Normality graph of residuals that belong to least square method

For the suitness of the predicted equation and normally distributed residuals, the residual values of predicted equation should not be autocorrelated. To achieve this, the sample autocorrelation function values of the residuals must be obtained for different lags. The autocorrelation over a series is measured by the autocorrelation function. Generally, the values of autocorrelation function is given by the sample autocorrelation function [42],

$$r_k = \frac{\sum_{t=1}^{n-k}(x_t - \bar{x})(x_{t-k} - \bar{x})}{\sum_{t=1}^{n}\left(x_t - \bar{x}\right)^2} \qquad k = 0,1,2.....,K \qquad (4.11)$$

where x_t is the observed value of the variable at time t, $\bar{x}$ is the mean of the observed variables, x_{t-k} is the observation value which is k time periods apart, k is the time lag and n is the number of observations, and r_k is the autocorrelation value for k time period.

For the values of lags, k=0 to 10 and n=100 sample autocorrelation functions have been calculated for the residual values of the predicted equation by using computer software, Excel. The data, applied to the sample autocorrelation functions, are given in Table A.1. in Appendix. To understand the residuals are autocorrelated or not, the distribution of them versus different lags should be checked by constructing a control

chart. It is also necessary to determine control limits so that if the autocorrelation values of residuals are out of control, it can be stated that the residual values are autocorrelated. The control limits of the control chart are [42],

$$UCL = 3.\frac{1}{\sqrt{n}} \tag{4.12}$$

$$LCL = -3.\frac{1}{\sqrt{n}} \tag{4.13}$$

where UCL and LCL are upper and lower control limits respectively and n is the number of sample. For n=100, the control limits are obtained as,

UCL = 0.3

LCL = -0.3

The change of sample autocorrelation function values, r_k, versus different lags is shown in Figure 4.19. According to the figure, it is observed that sample autocorrelation values of residuals are between control limits. This determines that the residual values are independent from each other. It can be concluded that there is no autocorrelation for residuals and residuals are normally and independently distributed.

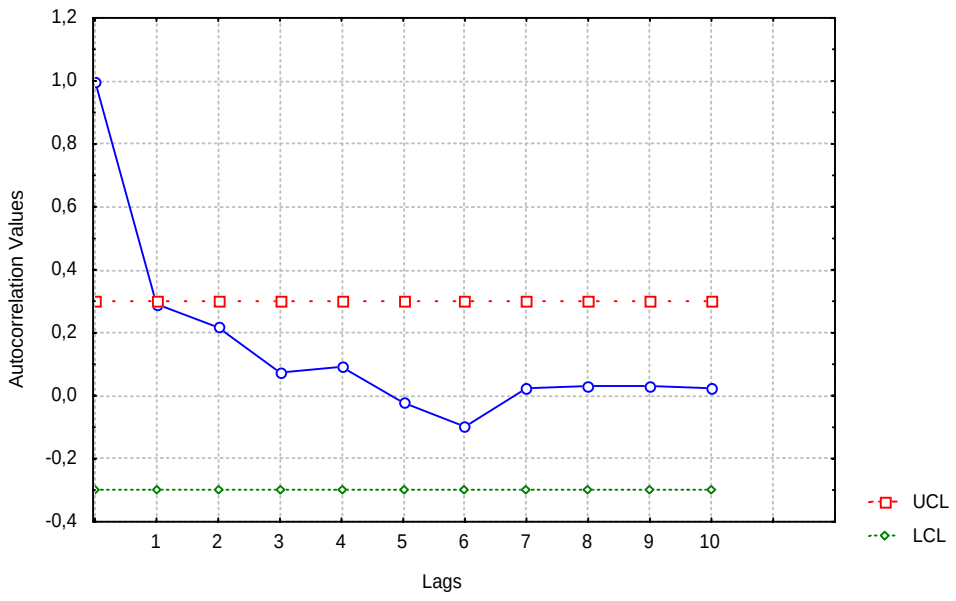

Figure 4.19. Sample autocorrelation values for the residuals

The quality of the predicted equation can be measured by coefficient of determination. The coefficient of determination is,

$$R^2 = 1 - \frac{\sum_{n=1}^{n} \varepsilon_n^2}{\sum_{n=1}^{n} (y_n - \bar{y})^2} = \frac{\sum_{n=1}^{n} (\hat{y}_n - \bar{y})^2}{\sum_{n=1}^{n} (y_n - \bar{y})^2} \qquad (4.14)$$

where ε_n is the residual value, y_n is the observed value of variable for that sample, $\bar{y}$ is the mean of observed values of variable, n is the number of sample and $\hat{y}_n$ is the predicted value of variable for that sample. Coefficient of determination represents the proportion of the sum of squares of the deviations of the y values about their predicted values that can be attributed to a linear relation between z and y.

R^2 is always between 0 and 1, because R is between –1 and +1. If R^2, the predicted equation passes through all the data. The observed DI% values in Table A.1. in Appendix were applied to to Equation (4.14). The value of R^2 was obtained as R^2=0.813 by using computer software, Excel. This means that 81.3% of the sample variation in density index values can be explained by this predicted equation [55]. Therefore it can be said that the predicted equation is suitable for the variables.

According to the predicted equation and the coefficient of determination, the density index values which show the amount of porosity in the material, are not only effected from hydrogen content. Samuel et. al. [52] explain that inclusions in the melt can lead to increase the porosity. As latter, E.L.Rooy [53] tells that shrinkage and hydrogen cause the porosity. Finally, Laslaz et. al. [54] inform that the number of the pores is increased in the case of oxidized metal for similar level of hydrogen content with all other parameters remaining constant.

Consequently, it can be determined that not only the hydrogen content but also the shrinkage, slag and inclusions have influences on the increasing of density index given as β_0 constant in the predicted equation. In the equation, the slope of the predicted line is given by β_1 constant. The effect of hydrogen content is obtained by this constant and the deviation from the zero value of density index is determined by β_0, defined by shrinkage, slag and inclusions.

4.3.3. Analysis of Variance for Single Factor

Analysis of variance for single factor is one of experimental design methods in order to understand the influence of one factor on the change of a process parameter.

This kind of research has been organized for determining the effect of degassing time on the hydrogen content in molten metal by using the data given in Table 4.1. Degassing time is chosen as the most important factor that can influence the hydrogen content in molten metal and also, it is controllable. The application was realized by a completely randomized single factor experiment with three levels. Each factor level has five observations. The role of randomization in this experiment is extremely important.

To analyze graphically, the data from a designed experiment is also an important factor. Figure 4.20. presents box plots of hydrogen content at the three degassing time levels. These plots indicate that changing the degassing time has a strong influence on hydrogen content [42].

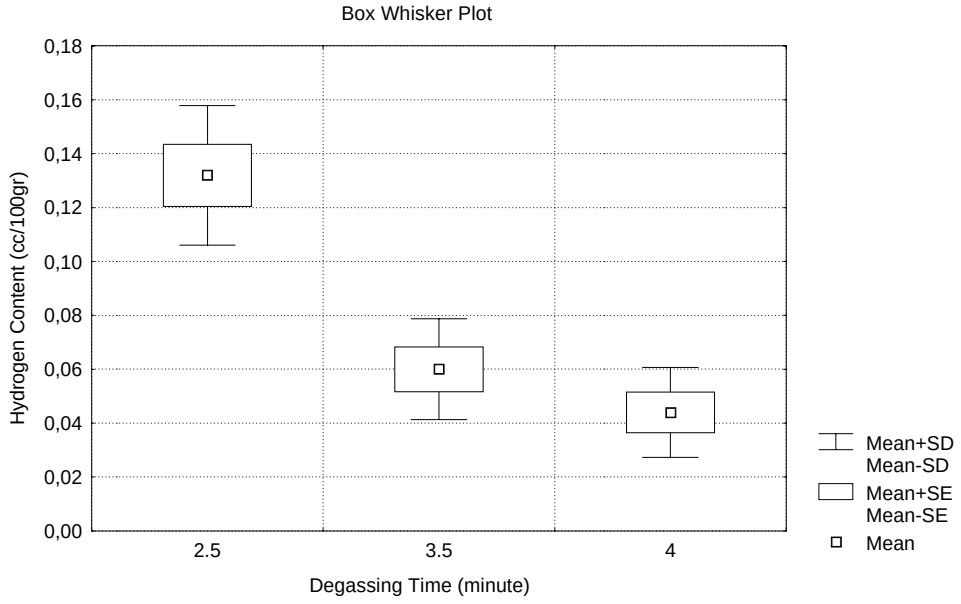

Figure 4.20. Change of hydrogen content values with different degassing time

Comparative box plots show the variability of the observations within a factor level and the variability between factor levels. By using analysis of variance with randomized single factor experiment, the effect of the factors on the process parameters can be achieved statistically. And, with the effective utilization of box plots and analysis of variance together, better results can be achieved.

The analysis of variance can be adapted to the data in Table 4.1. In the table, the hydrogen content observations are given according to the degassing time change for molten metal.

Table 4.1. Change of hydrogen content with degassing time factor

Degassing Time (minute)	Hydrogen Content (cc/100gr)					TOTAL	AVERAGE TOTAL
	1	2	3	4	5		
2,5	0,14	0,13	0,17	0,10	0,12	0,66	0,132
3,5	0,09	0,06	0,05	0,06	0,04	0,3	0,06
4	0,03	0,07	0,03	0,05	0,04	0,22	0,044
						1,18	0,236

To analyze variance for single factor, the equation

$$SS_T = SS_F + SS_E \tag{4.15}$$

is used where SS_T is the total sum of squares, SS_F is called the sum of squares due to the factor, and SS_E is called the sum of squares due to error.

For completeness, convenient computing formulas for the sum of squares are,

$$SS_T = \sum_{i=1}^{a}\sum_{j=1}^{n} y_{ij}^2 - \frac{y_{..}^2}{an} \tag{4.16}$$

and

$$SS_F = \sum_{i=1}^{a} \frac{y_{i.}^2}{n} - \frac{y_{..}^2}{an} \tag{4.17}$$

where a is the factor level, n is the number of observations, $y_{..}$,y_{ij} and $y_{i.}$ are the observation values. The error sum of squares is obtained by subtraction as,

$$SS_E = SS_T - SS_F \tag{4.18}$$

The sum of squares for the analysis of variance are computed for the data in Table 4.1,

$SS_T = (0.14)^2 + (0.13)^2 + ...+ (0.04)^2 – (1.18^2)/15$

The result is,

$SS_T = 0.12 – 0.0928 = 0.027$

Then,

$SS_F = (0.66^2 + 0.3^2 + 0.22^2)/5 – (1.18^2)/15$

It is obtained,

$SS_F = 0.1148 – 0.0928 = 0.022$

By using SS_T and SS_F,

$SS_E = SS_T - SS_F = 5x10^{-3}$

The ratio of a sum squares to its number of degrees of freedom is called a mean square; thus,

$$MS_F = \frac{SS_F}{a-1} \tag{4.19}$$

and

$$MS_E = \frac{SS_E}{a(n-1)} \tag{4.20}$$

It can be shown that the mean square error MS_E estimates the variance of the experimental error, σ^2. In addition, MS_F will tend to be greater than σ^2 if the factor level means are different. This leads to a statistical test based on the F distribution for equality of the factor means using the test statistic,

$$F_0 = \frac{MS_F}{MS_E} \tag{4.21}$$

If ,

$$F_0 \rangle F_{\alpha,\alpha-1,a(n-1)} \tag{4.22}$$

it may be concluded that the factor level means are different, where α is the probability of being out of confidence interval. Hence, mean squares for a=3 and n=5 are,

$MS_F = 0.022/2 = 0.011$

and

$MS_E = 5x10^{-3}/12 = 4.17x10^{-4}$

Then the test statistic is,

$$F_0 = \frac{MS_F}{MS_E} = \frac{0.011}{4.17x10^{-4}} = 26.37$$

For α=0.01, a=3 and n=5,

$F_{\alpha,\ a-1,\ a(n-1)} = F_{0.01,\ 2,\ 12} = 6.93$

Then,

$F_0 > F_{test}$

This result shows that degassing time effects the hydrogen content in the molten metal and hydrogen content in the molten metal decreases by increasing the degassing time.

Also, in order to reach the desired values of hydrogen content, optimum-degassing time should be chosen. The degassing must be made at lowest temperature

owing to the reason that as the temperature increases, the volume of the gas that passes for degassing increases [22]. Consequently, degassing process ought to be done at optimum temperature.

4.3.4. Changing of Hydrogen Content in Molten Metal with the Change of Molten Metal Temperature

As the hydrogen solubility increases with the increasing temperature of molten metal, the effect of molten metal temperature versus number of samples and hydrogen content was constructed in a graph as shown in the Figure 4.21. The change of hydrogen content in the molten metal, after the application of same degassing time, with the change of metal temperature as constructed by using the data given in Table A.2. in Appendix. As it can be seen from the figure, during the analyze of hydrogen content in the molten metal, especially from sample number 1 to 17 and 41 to 53 change of the hydrogen content is observed as being not in order. In these intervals, there become irregular trends for the hydrogen change.

However, between sample numbers 17 and 41, also, the temperature from 765°C to 775°C, the hydrogen content regularly changes. Therefore, it can be said that the hydrogen content change is between 765°C and 775°C temperature of molten metal. Between these temperature limits, the hydrogen content values are in the range of change between 0.15cc/100gr and 0.2 cc/100gr. In this range, there is stability in the hydrogen content of molten metal.

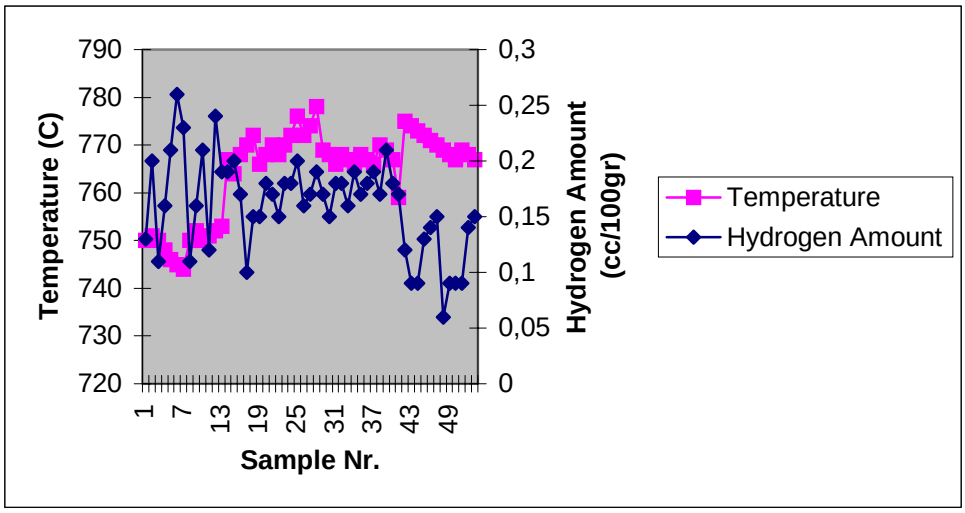

Figure 4.21. Effect of molten metal temperature on the hydrogen content value

For future studies, it can be suggested that fatigue and impact tests can be applied to cast Al wheels in order to determine the stress and fatigue properties of the wheel with different type of defects. Casting defects, especially gas pores and porosity, have important affects on the tensile strength and fatigue characteristics of the wheel. By applying fatigue testing, providing the simulation of actual road conditions and loading of the wheel, the influences of casting defects on the fatigue properties of cast Al wheel can be determined. Finite element method may be employed to analyze the stress levels and distribution in Al wheel corresponding to the loading conditions of the wheel and the size, location and type of the defects.

CHAPTER 5

CONCLUSIONS

In this study, cast Al wheel production of a big casting plant was investigated. Aim was to improve the quality of production by using the collected data from the process. The results obtained in this present study have allowed the following conclusions to be made:

1. To obtain more detailed and effective feedback control during the production of Al-wheel, a process model for the production line was constructed. By help of this diagram the causes of defects and remedies can be pointed immediately. Quality of the production is improved by determining process parameters. Fishbone diagrams were applied to the process and by using these diagrams parameters which have influence on the wheel production were clearly defined.
2. According to hydrogen content values which were used within this study and real-time radioscopic inspection results, the hydrogen content interval between 0.02cc/100gr and 0.27cc/100gr have the large number of the defected wheels as the hydrogen content values range between 0 and 0.35cc/100gr.
3. The investigation of the relation between the density index of gas holes and hydrogen content showed that there was a positive relation among these parameters. By using Least Square Method, it was shown that the predicted equation is true.
4. Analysis of variance for single factor shows that the hydrogen content in molten metal decreased by increased degassing time as expected.
5. Hydrogen content change in molten metal was in order between 765°C and 775°C temperature of molten metal. Between these temperature limits hydrogen content changed in the range of 0.15cc/100gr and 0.2cc/100gr as stable.

REFERENCES

[1] W.F.Smith, *Structure and Properties of Engineering Alloys*, (John Wiley, New York, 1993), p.218.

[2] R.Heine and P.Rosenthal, *Principles of Metal Casting*, (McGraw Hill, Tokyo, 1955), p.260.

[3] B.Webster, *Fundamentals of Foundry Technology*, (Porcullis Press, New York, 1980), p.252.

[4] H.Boyer and T.Gall, *Metals Handbook*, (American Society For Metals, Ohio, 1995), p.6.50.

[5] Y.Lakhtin, *Engineering Physical Metallurgy*, (MIR Publishers, Moscow, 1977), p.411.

[6] *Alloy Typical Applications*, (Society of Aluminum Manufacturers, Chicago, 1998), http://www.aluminum.org/casting alloys.html

[7] Shibata, Ryoichi, Watanabe and Rikizou, *High Toughness and High Strength Aluminum Alloy Casting*, US Patents Office, 1994), US5595615

[8] J.Evans, R.Hagan, W.Routh and R.Gibbs, *Aluminum Alloy and Method For Making Die Cast Products*, (US Patents Office, 1995), US 5573606

[9] Ramsden Company, *Mechanical Properties of Permanent Mold Casting Alloys*, (Ontario, 1999), http://www.ramsden.on.ca/alloys.htm

[10] Accuride Company, *Rim/Wheel Glossary*, (Montreal, 1998), http://www.accuride.com/index.htm

[11] Dooray, *Alloy Aluminum Wheel Production*, http://www.dooray.com/english/Plant-Wheel.htm

[12] Accuride Company, *Truck Wheels*, (Montreal, 1998), http://www.accuride.om/products.htm

[13] Hayes-Lemmerz Company, *Wheel Production*, (1997), http://www.hayes.com/products.htm

[14] Kato, Tadayoshi, Mizutani, Atsushi, Ichikava and Takashi, *Aluminum Wheel*, (US Patents Office, 1996), US 5803552

[15] D.Rogers and B.Koepke, "Heat Treating Aluminum Auto Parts", in *Advanced Materials and Processes*, 4(1997), 152

[16] Laihian Metalli Oy, *Comparison of Casting Methods,* http://www.jskanmetal.fi/eng/gb-valutavlu.html

[17] R.Heine and C.Loper, *Principles of Metal Casting*, (Mc Graw Hill, New York, 1967), p.259.

[18] Striko Company, *Shaft Type Melting Furnace*, http://www.striko.com

[19] L.P.Semersky, "Detecting Hydrogen Gas in Aluminum", in *Modern Casting*, 8(1983), 38-39

[20] Aluminum Casting Technology, (American Foundrymen Society, Illinois, 1997), p.1.

[21] Flinn, *Fundamentals of Metal Casting*, p.295.

[22] G.J. Davies, S*olidification and Casting*, (John Wiley & Sons, New York, 1973), p.166.

[23] H.Forberg, H.Chia and P.Keith, *Process For Degassing Aluminum And Aluminum Alloys*, (US Patents Office, 1975), US 3958981

[24] V. Tchernyi and V.Sapiyan, "New Low-Cost Environmentally Friendly Modifiers For Casting Aluminium Alloys", *Proceedings of the Symposium: International Metallurgy and Materials Congress*, (İstanbul, 2000), 469

[25] Pyrotekeurope, *Degassing and Refining Systems*, http://www.pyrotekeurope.com/products

[26] Twincity Die Casting, *Advantages of Die Casting*, http://www.twincity die casting. com

[27] American Die Casting Institute, *Types of Machines For Die Casting*, (1999), http://www.die casting.org/images.jpg

[28] Y.Kuang, *Facts About Die Casting Industry* (1998), http://www.ykd.com.tw/die-cast.htm

[29] H.Suzuki and S.Hashimoto, *Die Casting Method*, (US Patents Office, 1981), US 4380261

[30] J.Fields, M.Chu, L.Cisko and E.Eckert, *Die Casting Process and Equipment*, (US Patents Office, 1993), US 5370171

[31] N. Luther, *Metal Casting and Molding Processes*, (Luther & Associates, Tucson, 1996), p.1.

[32] J.D. Verhoeven, *Fundamentals of Physical Metallurgy*, (John Wiley & Sons, New York, 1975), p.217.

[33] T.B. Massalski, *Binary Alloy Phase Diagrams*, (ASM International, Chicago, 1990), p.211.

[34] *Solidification of Al-Si Alloys*, http://www.soton.ac.uk/~pasrl/al-si.htm

[35] I. Minkoff, *Solidification and Cast Structure*, (John Wiley & Sons, New York, 1986), p.210.

[36] A.G.Guy, *Physical Metallurgy*, (Addison Wesley, London, 1962), p.105.

[37] H.Aygün, "Identification of Casting Defects By Using Radiographic And Radioscopic Testing Methods", *Proceedings of the Symposium: 1st International NDT Symposium and Exhibition*, (Ankara, 1999), 185

[38] G.B. Suparta, R. Isaris and A. Moenir, "Restoration of Real Time Radiographic System For Industry in Indonesia ", *Proceedings of the Symposium: 15th WCNDT*, (Rome, 2000)

[39] J.G. Conley, J.Huang, J.Asada and K.Akiba, "Modeling the effects of cooling rate, hydrogen content, grain modifier on microporosity formation in Al A356 alloys", in *Materials Science & Engineering*, A285 (2000), 49-55

[40] R.C.Atwood, S.Sridhar, W. Zhang and P.D. Lee, "Diffusion-Controlled Growth Of Hydrogen Pores In Aluminium-Silicon Castings: In Situ Observation and Modelling", in *Acta Materialia*, 48(2000), 405-417

[41] J.P.Anson and J.E.Gruzleski, "The Quantitative Discrimination Between Shrinkage and Gas Microporosity In Cast Aluminum Alloys Using Spatial Data Analysis", in *Materials Characterization*, 335(1999), 319

[42] D.C. Montgomery, *Introduction To Statistical Quality Control*, (John Wiley & Sons, New York, 1997), p.1.

[43] D. Garwin, "Competing In The Eight Dimensions of Quality", in *Harward Business Review*, September-October (1987)

[44] YXLON International, "We make it visible CD", 2001

[45] M.Purschke, "Radioscopy-The Prevalent Inspection Technique of The Future", *Proceedings of the Symposium: 15th WCNDT*, (Rome, 2000)

[46] F.Brant, "The Use Of X-ray Inspection Techniques To Improve Quality and Reduce Costs", *Proceedings of the Symposium: 15th WCNDT*, (Rome, 2000)

[47] G.Box and T.Kramer, "Statistical Process Monitoring and Feedback", in *Technometrics*, 3(1992), 251

[48] G-Link, *Control Charts Module*, http://www.link.co.jp/English/csn/Control.htm

[49] PQ Systems, “Capability Analysis”, in *Statistics Articles*, (2000), http://www.pqsystems.com

[50] PQ Systems, “SPC and ISO/QS-9000”, in *Statistics Articles*, (2000), http://www.pqystems.com

[51] K.Ishikawa, *Guide To Quality Control*, (New York, 1982)

[52] A.M.Samuel and F.H.Samuel, “Porosity Factor In Quality Aluminum Castings”, in *AFS Transactions*, 11(1992), 657-666

[53] E.L.Rooy, “Preventing Porosity in Aluminum Castings”, in *Modern Casting*, 10(1992), 32-34

[54] G.Laslaz and P.Laty, “Gas Porosity and Metal Cleanliness in Aluminum Casting Alloys”, in *AFS Transactions*, 40(1991), 83-90

[55] W.Mendenhall and T.Sincich, *Statistics For Engineering and The Sciences,* (Mac Millan Publishing, New York, 1992), p.476.

APPENDIX

Table A.1. The data used for the examination of relation between hydrogen content and density index

Hydrogen	%Density Index	Hydrogen^2	Hydrogen * %Density Index	y^	y-y^
0,07	2,2	0,0049	0,154	3,6135	-1,4135
0,09	2,8	0,0081	0,252	4,3565	-1,5565
0,05	1,4	0,0025	0,07	2,8705	-1,4705
0,19	7,8	0,0361	1,482	8,0715	-0,2715
0,25	12,4	0,0625	3,1	10,3005	2,0995
0,24	11	0,0576	2,64	9,929	1,071
0,21	11,1	0,0441	2,331	8,8145	2,2855
0,24	10,8	0,0576	2,592	9,929	0,871
0,27	13,9	0,0729	3,753	11,0435	2,8565
0,26	13,6	0,0676	3,536	10,672	2,928
0,24	10,8	0,0576	2,592	9,929	0,871
0,26	12	0,0676	3,12	10,672	1,328
0,26	11,6	0,0676	3,016	10,672	0,928
0,24	9,6	0,0576	2,304	9,929	-0,329
0,11	6,2	0,0121	0,682	5,0995	1,1005
0,14	6,3	0,0196	0,882	6,214	0,086
0,1	5,9	0,01	0,59	4,728	1,172
0,16	10,1	0,0256	1,616	6,957	3,143
0,14	8,9	0,0196	1,246	6,214	2,686
0,14	10,2	0,0196	1,428	6,214	3,986
0,03	2,1	0,0009	0,063	2,1275	-0,0275
0,06	4,2	0,0036	0,252	3,242	0,958
0,09	2,2	0,0081	0,198	4,3565	-2,1565
0,04	1,8	0,0016	0,072	2,499	-0,699
0,05	2,5	0,0025	0,125	2,8705	-0,3705
0,04	1,4	0,0016	0,056	2,499	-1,099
0,04	2,8	0,0016	0,112	2,499	0,301
0,03	3,4	0,0009	0,102	2,1275	1,2725
0,06	2,8	0,0036	0,168	3,242	-0,442
0,05	2,6	0,0025	0,13	2,8705	-0,2705
0,04	2	0,0016	0,08	2,499	-0,499
0,03	1,6	0,0009	0,048	2,1275	-0,5275
0,04	1,2	0,0016	0,048	2,499	-1,299
0,03	1,5	0,0009	0,045	2,1275	-0,6275
0,04	3,5	0,0016	0,14	2,499	1,001
0,02	1,9	0,0004	0,038	1,756	0,144
0,03	1,9	0,0009	0,057	2,1275	-0,2275
0,04	3,6	0,0016	0,144	2,499	1,101
0,05	2,9	0,0025	0,145	2,8705	0,0295

0,02	1,8	0,0004	0,036	1,756	0,044
0,06	2,5	0,0036	0,15	3,242	-0,742
0,05	2,6	0,0025	0,13	2,8705	-0,2705
0,04	2,8	0,0016	0,112	2,499	0,301
0,04	3,1	0,0016	0,124	2,499	0,601
0,04	1,7	0,0016	0,068	2,499	-0,799
0,07	1,6	0,0049	0,112	3,6135	-2,0135
0,03	2	0,0009	0,06	2,1275	-0,1275
0,03	2,9	0,0009	0,087	2,1275	0,7725
0,04	2,8	0,0016	0,112	2,499	0,301
0,04	2,1	0,0016	0,084	2,499	-0,399
0,12	5,8	0,0144	0,696	5,471	0,329
0,18	8,7	0,0324	1,566	7,7	1
0,16	5,4	0,0256	0,864	6,957	-1,557
0,18	6,2	0,0324	1,116	7,7	-1,5
0,17	5,7	0,0289	0,969	7,3285	-1,6285
0,17	6,7	0,0289	1,139	7,3285	-0,6285
0,18	6,3	0,0324	1,134	7,7	-1,4
0,16	7,8	0,0256	1,248	6,957	0,843
0,19	7,6	0,0361	1,444	8,0715	-0,4715
0,14	7,3	0,0196	1,022	6,214	1,086
0,12	6,1	0,0144	0,732	5,471	0,629
0,09	5,4	0,0081	0,486	4,3565	1,0435
0,17	9,5	0,0289	1,615	7,3285	2,1715
0,09	7	0,0081	0,63	4,3565	2,6435
0,23	6	0,0529	1,38	9,5575	-3,5575
0,2	6,1	0,04	1,22	8,443	-2,343
0,26	8,1	0,0676	2,106	10,672	-2,572
0,16	7,3	0,0256	1,168	6,957	0,343
0,2	6,7	0,04	1,34	8,443	-1,743
0,15	6,4	0,0225	0,96	6,5855	-0,1855
0,23	8,1	0,0529	1,863	9,5575	-1,4575
0,04	0,9	0,0016	0,036	2,499	-1,599
0,16	7	0,0256	1,12	6,957	0,043
0,18	8,6	0,0324	1,548	7,7	0,9
0,19	7,5	0,0361	1,425	8,0715	-0,5715
0,19	8,1	0,0361	1,539	8,0715	0,0285
0,17	6,4	0,0289	1,088	7,3285	-0,9285
0,13	7,5	0,0169	0,975	5,8425	1,6575
0,17	8,1	0,0289	1,377	7,3285	0,7715
0,17	8	0,0289	1,36	7,3285	0,6715
0,25	9,6	0,0625	2,4	10,3005	-0,7005
0,04	1,8	0,0016	0,072	2,499	-0,699
0,12	7,3	0,0144	0,876	5,471	1,829
0,3	10,1	0,09	3,03	12,158	-2,058
0,12	8	0,0144	0,96	5,471	2,529
0,21	9	0,0441	1,89	8,8145	0,1855
0,2	7,6	0,04	1,52	8,443	-0,843

0,16	6,9	0,0256	1,104	6,957	-0,057
0,17	8,5	0,0289	1,445	7,3285	1,1715
0,24	9,6	0,0576	2,304	9,929	-0,329
0,33	9,8	0,1089	3,234	13,2725	-3,4725
0,2	8,4	0,04	1,68	8,443	-0,043
0,19	8,2	0,0361	1,558	8,0715	0,1285
0,22	7,3	0,0484	1,606	9,186	-1,886
0,04	1,8	0,0016	0,072	2,499	-0,699
0,19	8	0,0361	1,52	8,0715	-0,0715
0,16	7,9	0,0256	1,264	6,957	0,943
0,19	6,6	0,0361	1,254	8,0715	-1,4715
0,1	2,4	0,01	0,24	4,728	-2,328
0,12	4,7	0,0144	0,564	5,471	-0,771

Table A.2. The data for the determination of hydrogen content change with metal temperature

Sample Nr.	Temperature (°C)	Hydrogen
1	750	0,13
2	751	0,2
3	750	0,11
4	748	0,16
5	746	0,21
6	745	0,26
7	744	0,23
8	750	0,11
9	752	0,16
10	750	0,21
11	751	0,12
12	752	0,24
13	753	0,19
14	767	0,19
15	764	0,2
16	768	0,17
17	770	0,1
18	772	0,15
19	766	0,15
20	768	0,18
21	770	0,17
22	768	0,15
23	770	0,18
24	772	0,18
25	776	0,2
26	772	0,16
27	774	0,17
28	778	0,19
29	769	0,17
30	768	0,15
31	766	0,18
32	768	0,18
33	767	0,16
34	766	0,19
35	768	0,17
36	767	0,18
37	766	0,19
38	770	0,17
39	769	0,21
40	767	0,18
41	759	0,17
42	775	0,12

43	774	0,09
44	773	0,09
45	772	0,13
46	771	0,14
47	770	0,15
48	769	0,06
49	768	0,09
50	767	0,09
51	769	0,09
52	768	0,14
53	767	0,15